European Journal of Medicinal Chemistry 44 (2009) 2379–2391

Contents lists available at ScienceDirect

European Journal of Medicinal Chemistry

journal homepage: http://www.elsevier.com/locate/ejmech

Original article

Substituted quinazolines, part 3. Synthesis, *in vitro* antitumor activity and molecular modeling study of certain 2-thieno-4(3*H*)-quinazolinone analogs☆

Abdulrahman M. Al-Obaid [a], Sami G. Abdel-Hamide [a,*], Hassan A. El-Kashef [b], Alaa A.-M. Abdel-Aziz [a], Adel S. El-Azab [a], Hamad A. Al-Khamees [a], Hussein I. El-Subbagh [a,*]

[a] Department of Pharmaceutical Chemistry, College of Pharmacy, King Saud University, Riyadh 11451, Saudi Arabia
[b] Department of Pharmacology, College of Pharmacy, Mansoura University, Mansoura 35516, Egypt

ARTICLE INFO

Article history:
Received 5 May 2008
Received in revised form 18 July 2008
Accepted 1 September 2008
Available online 23 September 2008

Keywords:
Synthesis
2-Thieno-4(3*H*)-quinazolinones
Antitumor agents
Molecular modeling

ABSTRACT

The synthesis of some new 2-thieno-4(3*H*)-quinazolinone derivatives and their biological evaluation as antitumor agents using the National Cancer Institute (NCI) disease oriented antitumor screen protocol are investigated. Compounds 2-(2-thienylcarbonylamino)-5-iodo-*N*-(4-hydroxyphenyl)-benzamide (**16**), 2-(2-thieno)-6-iodo-3-phenylamino-3,4-dihydro-quina-zolin-4-one (**26**), and 2-(2-thieno)-4-[4-sulfonamidobenzylamino]-6-iodo-quinazoline (**42**), with GI_{50} values of 12.7, 10.3, 16.9 μM, respectively, proved to be the most active members in this study, as compared to the known drug 5-FU. Conformational analysis of the most active molecules using molecular modeling and QSAR techniques enabled the understanding of the pharmacophoric requirements for 2-thieno-quinzolinone derivatives as antitumor agents. These three quinazolinone analogs (**16**, **26**, **42**) could be considered as useful templates for future development to obtain more potent antitumor agents.

1. Introduction

Interests in quinazolines as anticancer agents have further increased since the discovery of raltitrexed (**1**) and thymitaq (**2**), (Chart 1). Both compounds proved to be thymidylate enzyme inhibitors [1–3]. 6-Arylamino-7-chloro-quinazoline-5,8-dione derivatives (**3**) showed potency against cultured human cancer cell line A549 (lung cancer), and stomach cancer SNU-638 [4–6]. Indolo-quinazolines **4**, **5** (Chart 1) proved active against a panel of human cancer cell lines [7]. Also, 4-anilinoquinazolines represent as a new class of antitumor drugs [2,3]. They inhibit the epidermal growth factor receptor (EGFR) tyrosine kinase overexpression through the inhibition of EGFR autophosphorylation and EGF-stimulated signal transduction [8,9]. Furthermore, quinazolines exert their antitumor activity through inhibition of the DNA repair enzyme system [7,10–14]. The present study aimed to synthesize and evaluate the biological activity of some new quinazoline derivatives as potential antineoplastic agents, as a continuation of our previous efforts [15,16]. A new series of quinazoline compounds are designed, in such a way to accommodate a thiophene ring at position 2-, sulphonamides, isothiocyanates, Schiff's bases or acylamides at position 3-, ether, thioether, amine bridges or sulphonamides at position 4- of the quinazoline ring. Thiophene [17], sulphonamide [18], thioether [19], isothiocyanate [18,20], Schiff's base and amide [20] functions are known to contribute to the enhancement of the antitumor activity.

2. Results and discussion

2.1. Chemistry

The reaction of 5-iodo-anthranilic acid (**6**) and 2-thiophenecarbonyl chloride (**7**) afforded the amide analog **8** which was then refluxed in acetic anhydride to obtain the key intermediate 2-(2-thieno)-6-iodo-4*H*-3,1-benzoxazin-4-one (**9**) (Scheme 1, Table 1). The latter compound was reacted with different aliphatic and aromatic amines in an attempt to obtain 3-substituted-quinazolin-4-ones in different reaction conditions, in all cases; the reaction afforded the diamides **10**–**12** and **14**–**18** instead. Attempts to cyclize the diamides **14**–**18** to the corresponding 4-(3*H*)-quinazolin-4-one using variety of reaction conditions, including fusion, were not successful. Compound **13** was obtained in very low yield by refluxing the corresponding diamide derivative **10** in thionyl chloride. The reaction of sulfa derivatives and homosulfanilamide with 3,1-benzoxozin-4-one **9** by fusion at high temperature afforded the corresponding quinazoline-4-one derivatives **19**–**22** (Scheme 1, Table 1). Reaction of **9** with the nucleophilic amino group of homosulfanilamide gave **23**. The benzoxazine derivative **9** was also reacted with hydroxylamine hydrochloride in dry pyridine to afford compound **24**. Condensation of **9** with various hydrazine derivatives afforded

☆ For parts 1 and 2, see Refs. [15,16].

* Corresponding authors. Department of Pharmaceutical Chemistry, College of Pharmacy, P.O. Box 2457, King Saud University, Riyadh 11451, Saudi Arabia. Tel.: +966 1 467 7394; fax: +966 1 467 6383.
E-mail address: subbagh@yahoo.com.

0223-5234/$ – see front matter © 2008 Elsevier Masson SAS. All rights reserved.
doi:10.1016/j.ejmech.2008.09.015

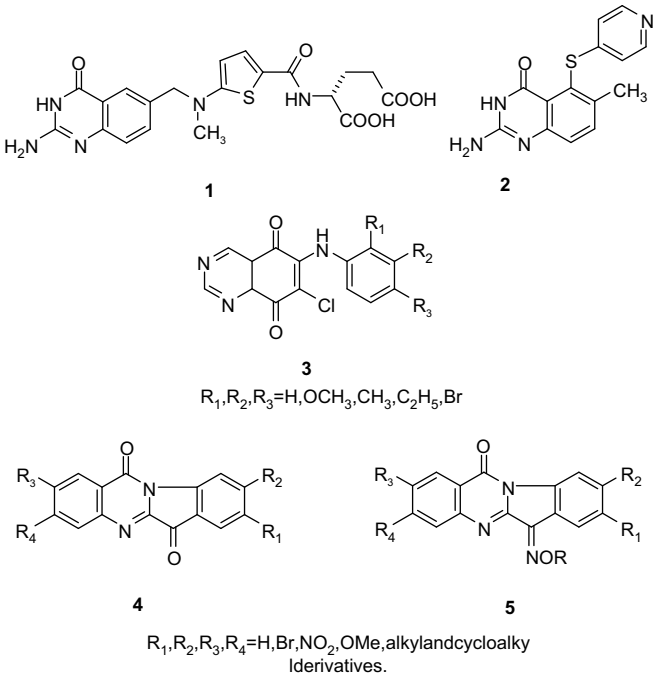

Chart 1.

compounds **25**–**29**. The intermediate **9** was also refluxed in formamide to afford 2-(2-thieno)-6-iodo-3,4-dihydro-quinazoline-4-one (**30**) which upon refluxing in dry xylene containing phosphorous pentasulfide afforded the corresponding 4-thione analog **31**. Alkylation of compound **31** with methyl and ethyl iodide afforded the 4-alkylthio analogs **32** and **33**, respectively (Scheme 2, Table 1). The 3-amino derivative **25** was reacted with phenylisocyanate or isothiocyanate in dry dioxane to afford the corresponding urea and thiourea derivatives **34**, **35**. Condensation of **25** with the appropriate aromatic aldehydes in glacial acetic acid afforded the arylidene derivatives **36** and **37.** Ethyl acetoacetate was refluxed with **25** in isopropanol to give the 3-oxo-butyrylamino derivative **38** (Scheme 2, Table 1). Alkylation of compound **30** with ethylbromoacetate in boiling acetone and anhydrous potassium carbonate afforded the *o*-alkyl derivative **39** which was reacted with hydrazine hydrate in absolute ethanol to form the hydrazide derivative **40**. The reaction of **30** with a mixture of phosphorous oxychloride and phosphorous pentachloride yielded the chloroquinazoline derivative **41** which was refluxed with homosulfanilamide or the appropriate sulfa drug in dry pyridine afforded compounds **42**–**45**, respectively (Scheme 3, Table 1).

2.2. Biological activity

The synthesized compounds (**8**–**45**, Schemes 1–3), were subjected to the NCI's *in vitro*, one dose primary anticancer assay, using a 3-cell line panel consisting of MCF-7 (breast), NCI-H460 (lung), and SF-268 (CNS) cancers. Compounds which reduce the growth of any one of the cell lines to 32% or less are passed on for evaluation in the full panel of 60 cell lines over a 5-log dose range [21–23]. Three response parameters, median growth inhibition (GI_{50}), total growth inhibition (TGI), and median lethal concentration (LC_{50}) were calculated for each cell line [24], using the known drug 5-Fluorouracil (5-FU) as a positive control. The NCI antitumor drug discovery screen has been designed to distinguish between broad-spectrum antitumor and tumor or subpanel-selective compounds [24]. In the present study, compounds **12**, **16**, **19**, **20**, **24**, **26**, **29**, **33**, **35**, **36**, **38**, **40**, **42** and **44** passed primary anticancer assay at an arbitrary concentration of 100 μM. Consequently, these active compounds were carried over and tested against a panel of 60 different tumor cell lines. The tested quinazoline analogs showed a distinctive potential pattern of selectivity as well as a broad-spectrum antitumor activity. With regard to sensitivity against individual cell lines (Table 2), compound **16** showed GI_{50} effectiveness against CNS SF-539 and melanoma UACC-257 cancer cell lines at concentration of <0.01 μM. Compound **26** showed activity against leukemia cell lines HL-60 (TB), K-562 and melanoma SK-MEL-2 with GI_{50} concentrations of 0.4, 0.3, and 0.3 μM, respectively. Compounds **16**, **19**, **29**, **40**, and **44** showed a remarkable activity against melanoma UACC-257 with GI_{50} concentrations of <0.01, 0.05, <0.01, <0.01, and 0.04 μM, respectively. Compound **35** showed GI_{50} effectiveness against leukemia K-562 at concentration of 0.02 μM. With regard to broad-spectrum antitumor activity, most of the tested compounds showed GI_{50}, TGI (MG-MID) values of <100 μM, against leukemia, non-small cell lung, colon, CNS, melanoma, ovarian, renal, prostate, and breast cancer subpanel cell lines (Tables 3 and 4). Compounds **16**, and **42** showed MG-MID values <100 μM at the three levels of activity, GI_{50}, TGI, and LC_{50} (Table 3), while compounds **19**, **20**, **24**, **26**, **29**, **35**, **38**, **40**, **42**, and **44** showed activity at GI_{50}, and TGI levels. Compound **33** was only active at the GI_{50} level. Compounds **12** and **36** proved to be inactive. Compounds **16**, **26**, and **42** are the most active members in this investigation, with GI_{50} values of 12.7, 10.3, and 16.9 μM, respectively. Compounds **16** and **26** are almost twofolds more active than the positive control 5-FU. When a full panel GI_{50} mean-graph (MG-MID) divided by a particular subpanel GI_{50} mean-graph, certain ratio will be obtained which helps to predict the selectivity of this compound toward this cell lines subpanel. Ratios of 3–6 are considered moderately selective and those with ratios of 6 or more are taken as selective [23]. Compound **26** proved to be selective toward prostate cancer cell lines with selectivity ratio of 6.4.

2.3. Structure–activity correlation

Structure–activity correlation of the synthesized compounds revealed that, in the diamide series **10**–**12** and **14**–**18**, aromatic substitution on the benzamide amide function, favors the activity

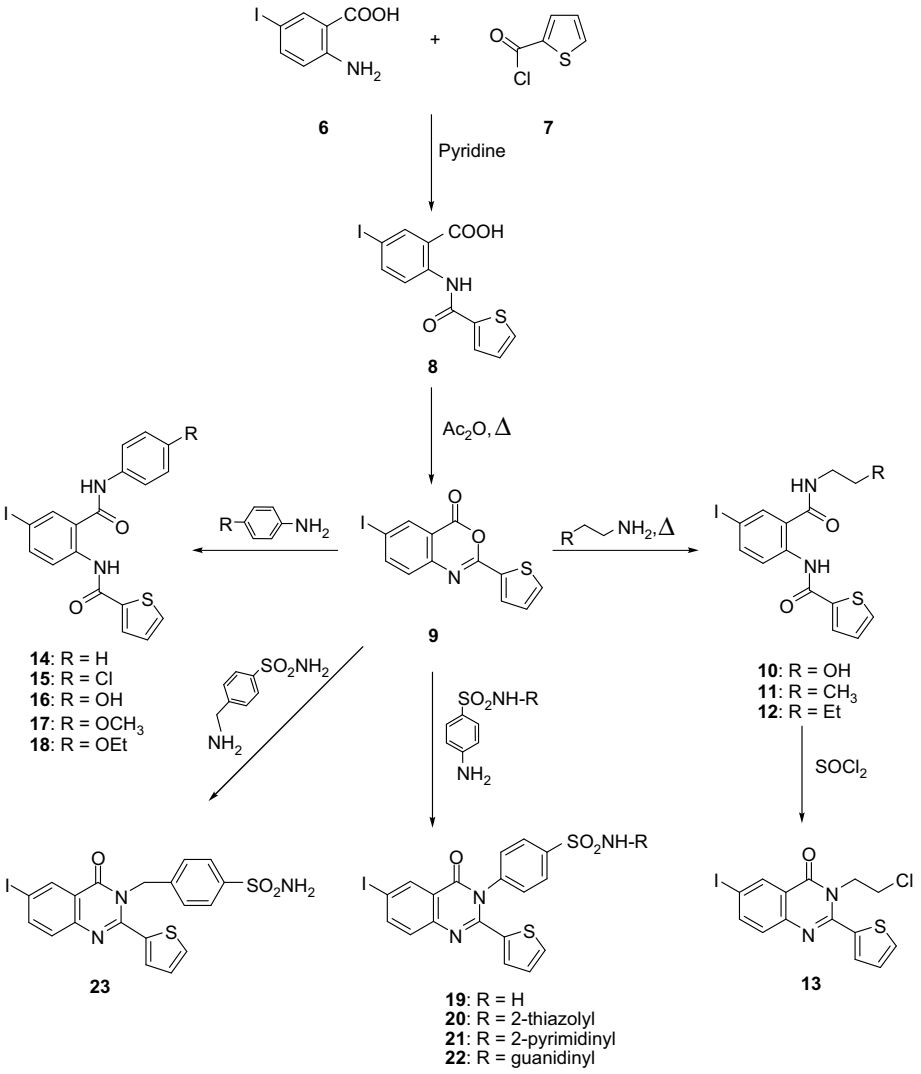

Scheme 1. Synthetic route for the preparation of the target compounds **10**–**23**.

rather than aliphatic substitution. This is obvious upon comparing compound **16** [*N*-(4-hydroxy phenyl), GI_{50} value 12.7 μM], and compound **10** [*N*-(2-hydroxy ethyl), value >100 μM]. In the sulfonamide series (**19**–**23**), compound **19** bearing unsubstituted sulfonamide function, which favors the antitumor activity (GI_{50} value of 24.9 μM), the introduction of 2-thiazolyl moiety to the sulfonamide group, markedly decreased the activity (**20**, $GI_{50} = 41.2$ μM). Introduction of a spacer methylene function produced the homosulfonamide **23** with total loss of activity. Moving the aromatic sulfonamide function from position 3- to position 4- of the quinazoline ring, favors the anticancer activity, as shown in compound **44** ($GI_{50} = 23.9$ μM) which is the positional isomer of **20** ($GI_{50} = 41.2$ μM), the same could be found in compound **42** ($GI_{50} = 16.9$ μM), and its positional isomer compound **23**. The introduction of the 3-amino function on the quinazoline ring produced the inactive compound **25**, conversion of the 3-amino group into aniline function yielded compound **26** ($GI_{50} = 10.3$ μM) as the most active member of this study. Replacing this 3-aniline function by benzamide, reduced the activity by threefold (compound **29**, $GI_{50} = 30.2$ μM). Aliphatic acylation of the 3-amino-quinazoline gave also the active compound **38** ($GI_{50} = 31.1$ μM). Further derivatization of the 3-amino group on **25** gave the thioureido analog **35** ($GI_{50} = 24.9$ μM), and the inactive azomethine compound **36**. Replacing the 3-amino group of **25** by 3-hydroxyl function (**24**, $GI_{50} = 41.1$ μM), markedly increased the activity. Conversion of the inactive ester **39** into its hydrazide **40** ($GI_{50} = 31.1$ μM), markedly increased the activity. The aforementioned information is in accordance with the pharmacophoric features essential for antitumor activity, deduced from the overall outcome of the molecular modeling study (next part).

2.4. Molecular modeling study

Modeling studies are required in order to construct molecular models that incorporate all reported experimental evidence. These models are necessary to obtain a consistent, more precise picture of the biological active molecules at the atomic level and furthermore, provide new insights that can be used to design novel therapeutic agents.

2.4.1. Conformational analysis

As an attempt to gain a better insight into the molecular structures of the active compounds **16**, **19**, **20**, **24**, **26**, **29**, **35**, **38**, **40**, **42** and **44**, and the inactive compounds **12**, **23**, **25**, **33** and **36**, conformational analysis has been performed by use of the MM^+ force-field [25] (calculations *in vacuo*, bond dipole option for electrostatics, Polak–Ribiere algorithm, and RMS gradient of 0.01 kcal/Å mol) as implemented in HyperChem 5.1 [26]. The most stable

Table 1
Physicochemical properties of the synthesized compounds **8**–**45**

Compd	Solvent	Yield (%)	MP (°C)	Molecular formulae
8	EtOH	77	260–262	$C_{12}H_8INO_3S$
9	Toluene	75	170–172	$C_{12}H_6INO_2S$
10	EtOH	65	210–212	$C_{14}H_{13}IN_2O_3S$
11	EtOH	70	144–146	$C_{15}H_{15}IN_2O_2S$
12	EtOH	75	130–132	$C_{16}H_{17}IN_2O_2S$
13	Dioxane	30	175–177	$C_{14}H_{10}ClIN_2OS$
14	EtOH	60	218–220	$C_{18}H_{13}IN_2O_2S$
15	EtOH	50	266–268	$C_{18}H_{12}ClIN_2O_2S$
16	Dioxane	65	235–237	$C_{18}H_{13}IN_2O_3S$
17	EtOH	70	221–222	$C_{19}H_{15}IN_2O_3S$
18	EtOH	75	170–172	$C_{20}H_{17}IN_2O_3S$
19	Dioxane	60	240–242	$C_{18}H_{12}IN_3O_3S_2$
20	EtOH	65	247–249	$C_{21}H_{13}IN_4O_3S_3$
21	Dioxane	70	310–311	$C_{22}H_{14}IN_5O_3S_2$
22	Dioxane	50	180–182	$C_{19}H_{14}IN_5O_3S_2$
23	EtOH	60	300–302	$C_{19}H_{14}IN_3O_3S_2$
24	EtOH	75	250–252	$C_{12}H_7IN_2O_2S$
25	EtOH	70	205–207	$C_{12}H_8IN_3OS$
26	EtOH	65	222–223	$C_{18}H_{12}IN_3OS$
27	EtOH	60	275–276	$C_{18}H_{11}ClIN_3OS$
28	MeOH	40	160–161	$C_{18}H_{10}IN_5O_5S$
29	Dioxane	60	213–214	$C_{19}H_{12}IN_3O_2S$
30	AcOH	66	330–331	$C_{12}H_7IN_2OS$
31	Benzene	40	225–226	$C_{12}H_7IN_2S_2$
32	EtOH	77	104–105	$C_{13}H_9IN_2S_2$
33	EtOH	72	110–112	$C_{14}H_{11}IN_2S_2$
34	Dioxane	61	190–191	$C_{19}H_{13}IN_4O_2S$
35	EtOH	73	295–296	$C_{19}H_{13}IN_4OS_2$
36	AcOH	75	236–237	$C_{19}H_{12}IN_3OS$
37	AcOH	79	221–222	$C_{20}H_{14}IN_3O_2S$
38	EtOH	56	134–136	$C_{16}H_{12}IN_3O_3S$
39	EtOH	75	110–112	$C_{16}H_{13}IN_2O_3S$
40	EtOH	70	210–212	$C_{14}H_{11}IN_4O_2S$
41	Toluene	60	129–130	$C_{12}H_6ClIN_2S$
42	AcOH	55	310–311	$C_{19}H_{15}IN_4O_2S_2$
43	AcOH	60	295–296	$C_{18}H_{13}IN_4O_2S_2$
44	AcOH	70	350–352	$C_{21}H_{14}IN_5O_2S_3$
45	AcOH	60	309–311	$C_{22}H_{15}IN_6O_2S_2$

conformer was fully optimized with AM1 semi-empirical molecular orbital calculation [27]. The global minimum was confirmed as true minimum not saddle point by the absence of negative eigen value of the Hessian through frequency calculation (Fig. 1) [28,29]. The calculation results classified these compounds into three different series, series-**A** including compounds **12** and **16**, series-**B** including compounds **24**–**26**, **29**, **35**, **36** and **38**, and series-**C** including compounds **19**, **20**, **23**, **33**, **40**, **42** and **44**. Each series has its own structural similarity which differs from one series to another, as indicated by their molecular parameters. Interestingly, the lowest energy-minimized structures of all series (**A**–**C**) exhibited a common arrangement of the aryl groups in position 3 (Fig. 1) and a critical distance of such aryl moiety from the quinazoline core. The optimal distance for the best biological activity was found in the range of 6–7 Å, lower or higher distance values lead to a decrease in activity, as indicated in Figs. 2 and 3.

2.4.2. Influence of lipophilic and steric factors

Further structural similarity evidence and its influence on biological activity were obtained from the QSAR-data using the conformations depicted in Fig. 1. QSAR studies showed an optimum hydrophobicity (log *P*) range of 2.4 (series-**A**), 3.5–5.5 (series-**B**) and 3.2–3.9 (series-**C**) for the active compounds, and log *P* range of 2.0 (series-**A**), 1.9–2.4 (series-**B**) and 2.9–3.0 (series-**C**) for the inactive compounds. Moreover, an optimum dipole moment range of 3.2 debye (series-**A**), 6.8–9.5 (series-**B**) and 3.1–6.3 (series-**C**) for the active compounds, and a dipole moment range of 2.9 (series-**A**), 4.0–5.8 (series-**B**) and 2.4–3.0 (series-**C**) for the inactive compounds. However, direct correlation could be established between the log *P* or the dipole moment and antitumor activity among each series but it seems to be difficult to correlate one series to another. These results indicate that the activity of the compound depends on their lipophilicity. It becomes apparent that log *P* or dipole moment values are not the sole predicting factor for biological activity in this study [30]. In addition, despite the variation of the molecular shapes of these series; measurements of global molecular parameters such as surface area, volume, and refractivity, also reflect their similarity. The biological inefficacy of the inactive compounds could be attributed to the difficulty to cross the lipid biological membranes due to their physicochemical properties.

2.4.3. Flexible alignment

Flexible alignment is an application for flexibly aligning small molecules. The method accepts as input a collection of small molecules with 3D coordinates and computes a collection of alignments. Each alignment is given a score that quantifies the quality of the alignment in terms of both internal strain and overlap of molecular features. Often, atomic-level details of the structures of pharmaceutically relevant receptors are not available. In such cases, 3D alignment (or superposition) of putative ligands can be used to deduce structural requirements for biological activity. Methodologies based upon 3D alignment for finding biologically active ligands generally make use of the qualitative assumption that if two ligands have similar biological activity [31–33].

To probe similarity between the three-dimensional structures of active compounds **16**, **26** and **42**, flexible alignment was employed. Our initial approach was to employ MOE/flexible alignment [34] to automatically generate superpositions of the compounds under investigation with minimal user bias. Using MOE/MMFF94, 200 conformers of each compound were generated and minimized with a distance-dependant dielectric model. A low energy set of 100 was selected for further analysis. Conformations of compound **26** were generated using distance geometry and optimized with MMFF94 [35]. Nine low energy, maximally dissimilar structures were selected for comparison to the other compounds **16** and **42**. After assigning MMFF94 charges to all molecules, flexible alignment was employed to scan and rank overlays of compounds **16**, **26** and **42** based on steric, electrostatic field, hydrophobic areas overlap, hydrogen bond donors and acceptors overlap. From the top scoring superposition, several sets most consistent with the structure–activity relationships of the three antitumor compounds were selected and subjected to more refined searching using MOE/flexible alignment module [34]. Since the molecules are highly flexible, the limited set of conformers used in the analysis was not capable of achieving complete atom-to-atom superposition. A further refinement was generated (Fig. 4, left panel) by constraining the functional group mapping suggested from the initial alignment. The calculated energy difference between the native conformers derived from the flexible alignment and the final conformers in Fig. 4 is minimal. In fact, the refined structure of compound **26** was 0.2 kcal/mol lower in energy than the starting structure, and compounds **16** and **42** was 1.0 and 0.5 kcal/mol lower, respectively. A common feature of the MOE-generated alignments is the superposition of the aryl groups of the compounds with a slight deviation (0.2–1.0 Å) Moreover, the NH fragment of the compound **26** maps to the NH fragment of other the compounds **16** and **42** (0.2–0.9 Å). The thiophene ring and quinazoline nucleus align fairly well for the three compounds with almost complete superposition of the thiophene rings of compounds **26**, **16** and **42** (0.4 Å).

By the same way, antitumor compounds **26**, **16** and inactive compound **36** were subjected to flexible alignments. As shown in Fig. 4 (right panel), all active compounds have the same feature of alignment as we described above showing four points of similarities: thiophene moiety, quinazoline core, NH group directly

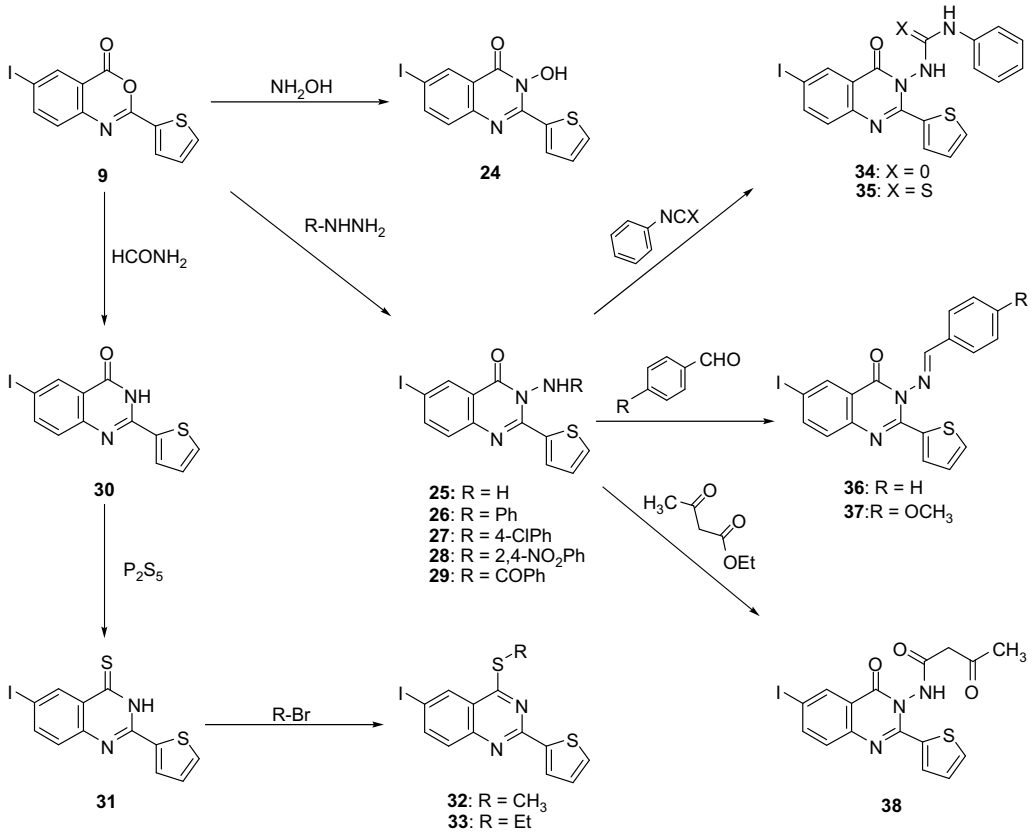

Scheme 2. Synthetic route for the preparation of the target compounds **24**–**38**.

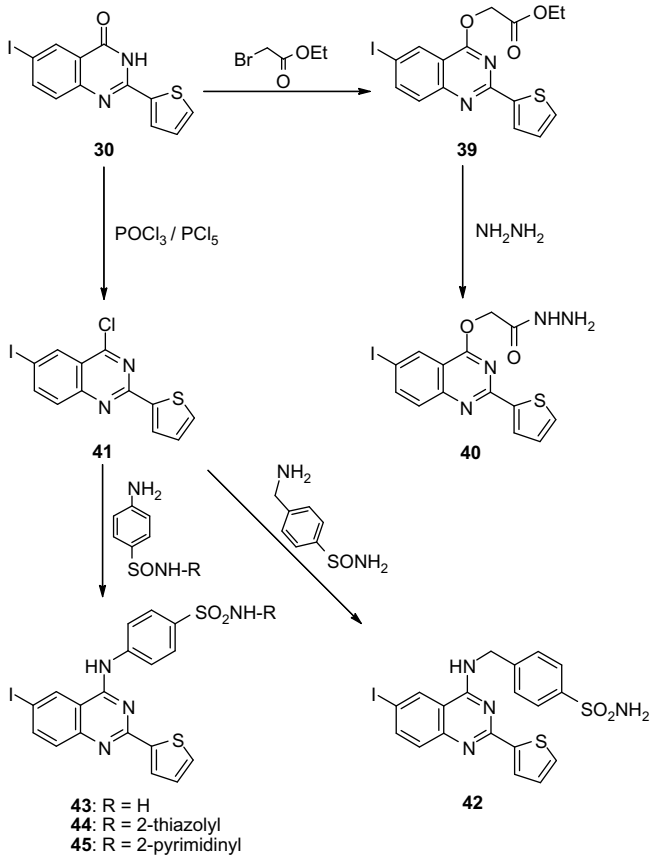

Scheme 3. Synthetic route for the preparation of the target compounds **39**–**45**.

attached to quinazoline moiety as hydrogen bond donor, and aromatic ring attached to such NH moiety. Analysis of inactive molecule is an important step to understand the essential features for a given activity. It is clear that compound **36** was flexibly aligned in a different manner when compared to the active compounds explaining why such compound was void of antitumor activity and showing the importance of both NH moiety and the aromatic ring attached to this NH group for activity (Fig. 4).

2.4.4. Pharmacophore prediction [33]

For pharmacophore generation and prediction, compound **26** (Figs. 5 and 6) served as the reference to which all conformations of each analog were aligned. All structures were built *de novo* using 2D/3D editor sketcher in MOE [34]. Conformational models were calculated using a 15 kcal energy cut off (minimization convergence criteria during conformational analysis: energy convergence = 0.01 kcal/mol, gradient convergence = 0.01 kcal/mol). The number of conformers generated for each substrate was limited to a maximum of 150. All molecules with their associated conformations were regrouped including the biological data. Hypothesis generation was performed using low energy conformers of the molecules. After assignment of possible pharmacophore elements for each analog the calculation and analysis were carried out using the MOE program [34] and a superposition of the molecules, including the assigned elements, was attempted (Figs. 5 and 6). Several runs of calculation were repeated to generate pharmacophore maps. For each run a distinct number of specified pharmacophore elements were adapted. All adapted models showed that the donor atoms of the NH fragments as hydrophilic element and the aryl moieties as hydrophobic element were well superimposed within the set distance tolerance. This confirms the important role of the hydrophilic and hydrophobic moieties for recognition and binding to receptor sites.

Table 2
Growth inhibitory concentrations (GI_{50}, TGI) and lethal concentration (LC_{50}) of some selected *in vitro* tumor cell lines[a] (μM)

Compd[b]	Activity	Leukemia				CNS	Melanoma		Breast	
		CCRF-CEM	HL-60 (TB)	K-562	RPMI-8226	SF-539	SK-MEL-2	UACC-257	MCF-7	T-47D
16	GI_{50}	nt[c]	8	24	3	<0.01	16	<0.01	12	2
	TGI	nt	37	[d]	18	15	30	22	33	11
	LC_{50}	nt	[d]	[d]	57	62	57	[d]	94	50
19	GI_{50}	41	20	37	25	nt	22	0.05	23	19
	TGI	[d]	64	[d]	62	nt	48	19	65	44
	LC_{50}	[d]	[d]	[d]	[d]	nt	[d]	[d]	[d]	99
26	GI_{50}	51	0.4	0.3	5	34	0.3	32	2	nt
	TGI	[d]	[d]	23	[d]	[d]	2	[d]	[d]	nt
	LC_{50}	[d]	[d]	[d]	[d]	[d]	[d]	[d]	[d]	nt
29	GI_{50}	39	34	44	23	30	24	<0.01	23	11
	TGI	[d]	[d]	[d]	58	[d]	69	31	[d]	38
	LC_{50}	[d]	[d]	[d]	[d]	[d]	[d]	[d]	[d]	[d]
35	GI_{50}	21	1	0.02	19	34	nt	17	29	3
	TGI	61	22	10	52	[d]	nt	66	88	17
	LC_{50}	[d]	[d]	75	[d]	[d]	nt	[d]	[d]	[d]
40	GI_{50}	20	38	37	16	nt	25	<0.01	16	2
	TGI	88	[d]	[d]	39	nt	71	[d]	89	22
	LC_{50}	[d]	[d]	[d]	97	nt	[d]	[d]	[d]	[d]
42	GI_{50}	22	30	37	19	11	18	14	0.6	0.2
	TGI	60	[d]	[d]	50	31	33	28	16	18
	LC_{50}	[d]	[d]	[d]	[d]	85	61	54	[d]	82
44	GI_{50}	2	32	38	1	32	22	0.04	26	15
	TGI	4	80	[d]	3	60	47	28	[d]	51
	LC_{50}	9	[d]	[d]	8	[d]	[d]	95	[d]	[d]

[a] Data obtained based on the NCI's *in vitro* disease oriented human tumor cell lines screening protocol.
[b] Compounds passed the *in vitro* one dose primary anticancer screen.
[c] nt, compound not tested.
[d] Values > 100 μM.

Models for **26** and its analogs **16** and **42** (Fig. 5) possess pharmacophore elements in the aromatic ring attached to NH group (as a hydrogen bond donor) which is out of the thiophene plane as well as quinazoline core in the same plane of thiophene ring. In contrast, model for **36** (Fig. 6) showed common elements only in thiophene fragment attached to quinazoline core. Since the arylamino part of compound **26** plays an important role in activity, model **36** was excluded from further considerations. Therefore, model **26** was considered as the representative pharmacophore map of the antitumor activity.

According to the pharmacophore generated by MOE [34] the minimal structural requirements for antitumor activity consist of an aromatic ring (hydrophobic region) attached to NH fragment (H-bonding donor region), and a hydrophobic region represented by quinazoline core and thiophene fragment. For all the active molecules, reasonable nonbonded distances among the aromatic ring, quinazoline core and the thiophene centroid align on the predicted pharmacophore maps were found (Figs. 2, 3, and 5). This pharmacophoric assumption was in consistence with biological data.

Table 3
Median growth inhibitory concentration (GI_{50}, μM) of *in vitro* subpanel tumor cell lines

Compd	Subpanel tumor cell lines[a]									MG-MID[b]
	I	II	III	IV	V	VI	VII	VIII	IX	
12	83.8 ± 10.2	96.0 ± 2.6	[c]	>100	[c]	[c]	[c]	[c]	>100	[c]
16	11.5 ± 3.1	13.5 ± 0.9	15.2 ± 1.4	12.2 ± 3.1	11.1 ± 2.0	13.3 ± 1.1	13.2 ± 1.3	8.7 ± 1.9	11.9 ± 2.2	12.7 ± 0.65
19	35.3 ± 4.7	24.0 ± 1.3	24.8 ± 2.7	30.3 ± 3.8	17.6 ± 2.6	23.5 ± 2.0	24.7 ± 1.6	22.7 ± 3.9	23.3 ± 2.7	24.9 ± 1.1
20	54.0 ± 4.7	38.7 ± 8.2	44.7 ± 9.3	41.4 ± 11.9	45.2 ± 10.1	46.5 ± 9.9	34.2 ± 4.0	32.9 ± 5.5	34.8 ± 10.0	41.2 ± 2.8
24	34.3 ± 3.1	33.2 ± 3.7	45.8 ± 9.3	33.2 ± 3.8	57.3 ± 7.4	32.1 ± 4.8	49.8 ± 9.3	39.9 ± 12.2	39.4 ± 4.0	41.1 ± 2.4
26	12.7 ± 7.8	8.6 ± 3.0	6.5 ± 2.0	16.3 ± 5.6	8.5 ± 4.6	8.6 ± 4.7	19.7 ± 9.7	1.61	5.9 ± 4.11	10.3 ± 1.8
29	33.9 ± 3.6	25.6 ± 2.3	35.4 ± 6.2	27.4 ± 2.2	35.5 ± 10.9	27.4 ± 4.6	32.1 ± 2.5	27.2 ± 6.6	24.5 ± 4.8	30.2 ± 1.8
33	–	84.2 ± 10.4	94.6 ± 3.9	[c]	[c]	85.2 ± 14.8	[c]	[c]	71.4 ± 18.1	90.6 ± 3.4
35	11.5 ± 4.4	24.0 ± 4.1	29.5 ± 2.1	29.2 ± 6.1	23.1 ± 3.1	21.5 ± 3.2	32.5 ± 5.1	25.8 ± 1.5	19.4 ± 4.3	24.9 ± 1.5
36	63.4 ± 22.3	[c]	[c]	[c]	90.3 ± 6.8	[c]	[c]	[c]	[c]	[c]
38	38.5 ± 4.8	27.5 ± 3.2	28.1 ± 2.8	27.9 ± 4.5	37.7 ± 9.3	40.9 ± 12.4	28.9 ± 3.8	20.6 ± 6.0	24.9 ± 3.8	31.1 ± 2.1
40	25.4 ± 4.1	19.4 ± 1.1	24.3 ± 2.9	20.7 ± 2.5	19.4 ± 3.1	22.3 ± 2.0	23.1 ± 2.1	23.5 ± 1.8	18.7 ± 4.3	21.5 ± 0.95
42	23.9 ± 3.2	14.7 ± 1.6	16.7 ± 2.7	18.2 ± 1.6	16.0 ± 0.88	15.7 ± 2.0	13.6 ± 2.9	17.1 ± 2.2	12.3 ± 4.2	16.9 ± 0.94
44	21.7 ± 6.7	23.3 ± 2.6	24.3 ± 2.6	27.7 ± 3.3	18.9 ± 3.0	25.8 ± 2.3	28.3 ± 1.1	13.9 ± 7.9	25.9 ± 4.2	23.9 ± 1.1
5-FU	15.09 ± 3.8	[c]	8.37 ± 2.6	72.07 ± 0.01	70.6 ± 41.5	61.4 ± 20.2	45.6 ± 28.8	22.7 ± 16.8	76.4 ± 29.1	22.6 ± 3.6

[a] I, leukemia; II, non-small cell lung cancer; III, colon cancer; IV, CNS cancer; V, melanoma; VI, ovarian cancer; VII, renal cancer; VIII, prostate cancer; IX, breast cancer.
[b] GI_{50} full panel mean-graph midpoint (μM).
[c] Values > 100 μM.

Table 4
Total growth inhibitory concentration (TGI, μM) of *in vitro* subpanel tumor cell lines

Compd	Subpanel tumor cell lines[a]									MG-MID[b]
	I	II	III	IV	V	VI	VII	VIII	IX	
12	[c]	[c]	[c]	[c]	[c]	[c]	[c]	[c]	[c]	[c]
16	60.6 ± 14.9 (91.0 ± 7.0)	33.1 ± 2.8 (74.6 ± 5.1)	34.5 ± 6.0 (74.6 ± 5.1)	32.4 ± 5.6 (77.6 ± 7.9)	26.9 ± 1.5 (63.8 ± 5.9)	35.4 ± 5.3 (72.5 ± 11.3)	29.3 ± 2.4 (64.1 ± 6.2)	21.1 ± 1.4 (45.8 ± 1.5)	36.8 ± 7.8 (79.4 ± 9.2)	35.0 ± 2.4 (71.8 ± 2.6)
19	87.7 ± 7.7	61.3 ± 6.2	59.3 ± 10.3 (87.1 ± 6.7)	73.8 ± 7.0	43.0 ± 4.1	65.1 ± 9.6	64.1 ± 9.1 (94.1 ± 4.4)	58.9 ± 23.0	62.5 ± 10.5	63.3 ± 3.1
20	[c]	89.5 ± 5.5	94.6 ± 5.3	87.7 ± 9.1	84.8 ± 8.35	[c]	84.3 ± 7.9	[c]	88.3 ± 6.0	90.4 ± 2.2
24	[c]	91.2 ± 4.7	[c]	94.4 ± 5.6	97.1 ± 2.8	87.9 ± 11.3	[c]	98.4 ± 1.5	[c]	93.3 ± 2.1
26	87.1 ± 12.0	88.0 ± 5.7	79.2 ± 14.3	81.9 ± 13.0	85.9 ± 14.0	80.1 ± 15.3	93.1 ± 6.8	[c]	[c]	86.7 ± 3.8
29	71.5 ± 14.7	75.3 ± 7.1	90.0 ± 5.9	85.8 ± 7.2	62.1 ± 8.4	74.4 ± 10.8	86.7 ± 7.8	73.3 ± 26.6	72.5 ± 12.4	77.6 ± 3.2
33	[c]	[c]	[c]	[c]	[c]	[c]	[c]	[c]	[c]	[c]
35	38.5 ± 9.5	75.2 ± 8.0	84.0 ± 7.9	81.4 ± 12.5	62.8 ± 16.4	77.5 ± 10.5	84.8 ± 7.7	76.2 ± 23.8	60.3 ± 13.0	72.0 ± 3.6
36	[c]	[c]	[c]	[c]	[c]	[c]	[c]	[c]	[c]	[c]
38	[c]	86.4 ± 7.2	90.9 ± 9.1	89.1 ± 10.9	85.3 ± 7.1	93.6 ± 6.4	85.1 ± 8.2	[c]	82.1 ± 7.6	88.6 ± 2.6
40	80.5 ± 10.8	59.6 ± 5.4	66.9 ± 9.6	62.1 ± 7.8	51.1 ± 4.3	72.5 ± 9.8	71.1 ± 8.1	75.3 ± 24.6	64.7 ± 13.3	65.9 ± 3.0
42	72.3 ± 10.2	37.0 ± 3.2 (82.2 ± 6.1)	37.3 ± 7.9 (66.4 ± 6.5)	42.4 ± 4.3 (89.0 ± 3.8)	30.5 ± 1.5 (58.3 ± 2.7)	42.6 ± 4.9 (89.1 ± 4.9)	36.1 ± 7.3 (88.1 ± 5.1)	41.8 ± 11.5 (80.8 ± 19.2)	32.1 ± 10.6 (80.8 ± 8.1)	40.5 ± 2.6 (79.3 ± 2.7)
44	59.2 ± 18.2 (69.4 ± 19.3)	65.2 ± 8.9 (92.4 ± 5.8)	61.1 ± 11.2 (87.3 ± 5.0)	68.3 ± 8.6	45.5 ± 4.8 (92.1 ± 4.6)	68.9 ± 8.3	79.6 ± 6.8	35.9 ± 17.0 (73.0 ± 27.0)	74.9 ± 11.2	63.8 ± 3.5
5-FU	[c]	[c]	[c]	[c]	[c]	[c]	[c]	[c]	[c]	[c]

[a] For subpanel tumor cell lines, see footnote a of Table 3.
[b] TGI full panel mean-graph midpoint (μM).
[c] Compounds showed values > 100 μM. Median lethal concentration (LC_{50}, μM) of *in vitro* subpanel tumor cell lines and LC_{50} full panel mean-graph midpoint (μM) are shown in parentheses.

3. Conclusion

Compounds 2-(2-thienylcarbonylamino)-5-iodo-*N*-(4-hydroxy phenyl)-benzamide (**16**), 2-(2-thieno)-6-iodo-3-phenylamino-3,4-dihydro-quinazolin-4-one (**26**), and 2-(2-thieno)-4-[4-sulfonamidobenzylamino]-6-iodo-quinazoline (**42**), with GI_{50} values of 12.7, 10.3, 16.9 μM, respectively, proved to be the most active members in this study, as compared to the known drug 5-FU. These three quinazoline analogs could be considered as useful templates for future development to obtain more potent antitumor agent(s). Flexible alignment was conducted on the basis of experimental data from which four featured pharmacophore model was developed. The model was mapped onto the antitumor molecules and compared with nonactive compounds. This pharmacophore model could be very useful for the virtual screening in the development of new antitumor agents. The overall outcome of this model revealed that: (i) the quinazolinone ring is a satisfactory backbone for antitumor activity, (ii) the presence of aryl moiety at the 3-amino position is necessary for the activity as hydrophobic region, (iii) the aryl group at position 3- should be about 6.0–7.0 Å apart from the quinazolinone core (Figs. 2 and 6), (iv) introduction of spacer group, between 3-amino-quinazolinone ring and aryl moiety decreases the activity, such as 3-benzoylamino moiety, (v) the presence of one hydrogen atom attached to 3-amino group as a hydrogen bonding donor is essential for activity and its removal through formation of benzylidene moiety diminishes the activity (Figs. 2 and 6), (vi) the presence of sulfonamide group located on the 3-aryl moiety of quinazoline is necessary as H-bond region (Figs. 3 and 5) (vii) the

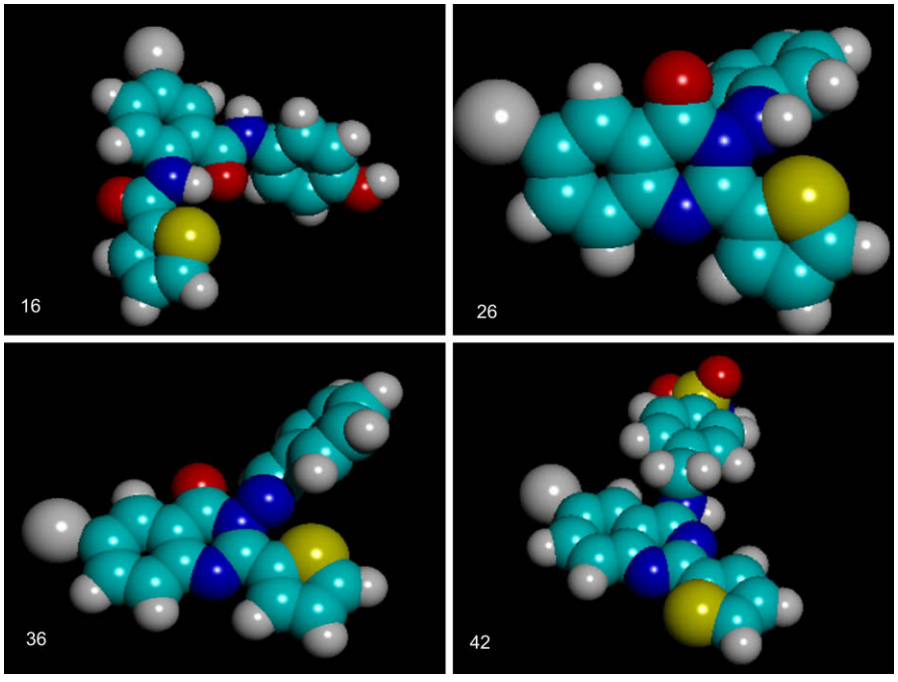

Fig. 1. Lowest energy conformers of the most active compounds **16**, **26**, **42** and the inactive compound **36** as representative examples with CPK rendering.

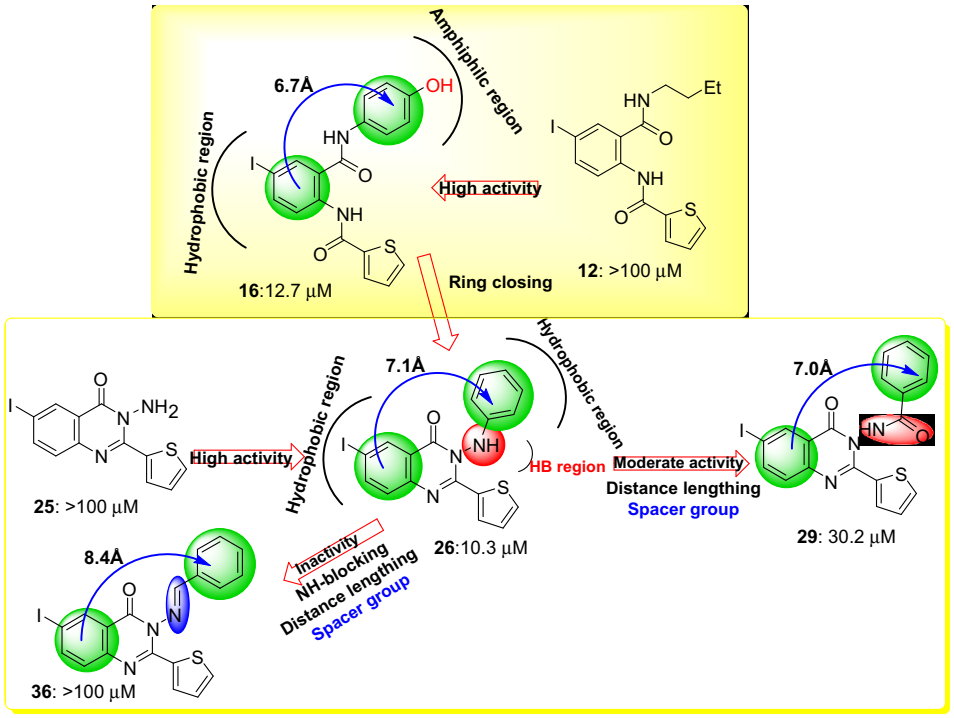

Fig. 2. 2D-pharmacophoric design of 3-arylquinazoline (red colors represent the HB regions and green colors represent hydrophobic regions and blue colors represent spacer moiety). (For interpretation of the references to color in this figure legend, the reader is referred to the web version of this article.)

free sulfonamide function improves the activity, while the substituted sulfonamide blunts this action and (viii) regioisomerization of the arylsulfonamide group from position 3- to position 4- of the quinazoline increases the antitumor activity as indicated upon comparing compounds **23** and **42**.

4. Experimental

Unless otherwise specified all chemicals were of commercial grade, used without further purification and were obtained from Aldrich Chemical Co. (Milwaukee, WI). Solvents used for work ups were dried over $MgSO_4$, filtered and removed on a rotary evaporator. Elemental analyses were performed at College of Pharmacy, King Saud University, Central Laboratory. ^1H NMR spectra were obtained at 500 MHz by JEOL instrument using TMS as internal standard. Thin layer and flash chromatographies were performed using E. Merck Silica gel (230–400 mesh). Preparative thin layer chromatography was performed on Harrison model 7924A chromatotron using Analtech silica gel GF rotors. All modeling studies were conducted with HyperChem 5.1 package from Hypercube [26]. Flexible alignment and 3D-pharmacophore prediction were generated by MOE 2007.09 software [34].

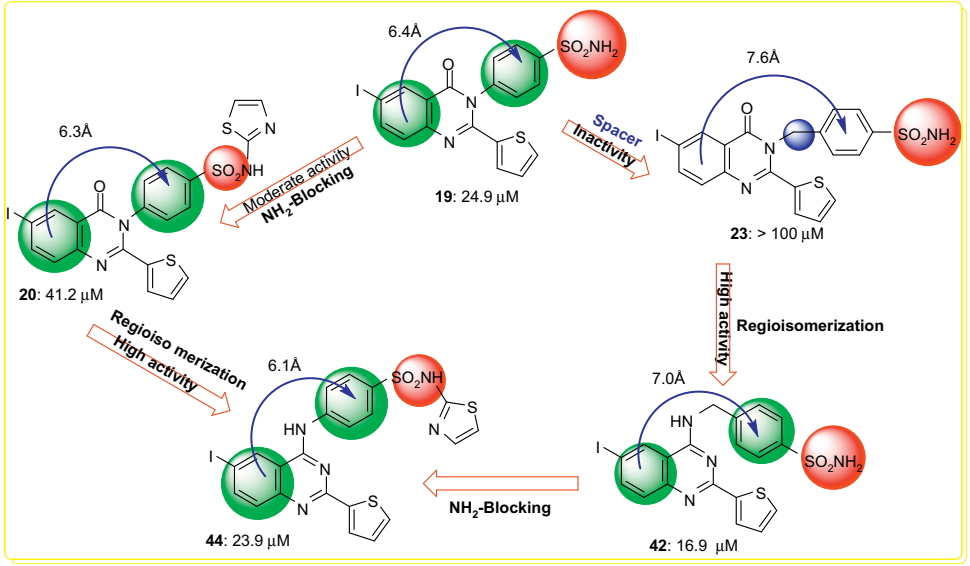

Fig. 3. 2D-pharmacophoric design of the sulfonamido-quinazoline (red colors represent the HB regions and green colors represent hydrophobic regions and blue colors represent spacer moiety). (For interpretation of the references to color in this figure legend, the reader is referred to the web version of this article.)

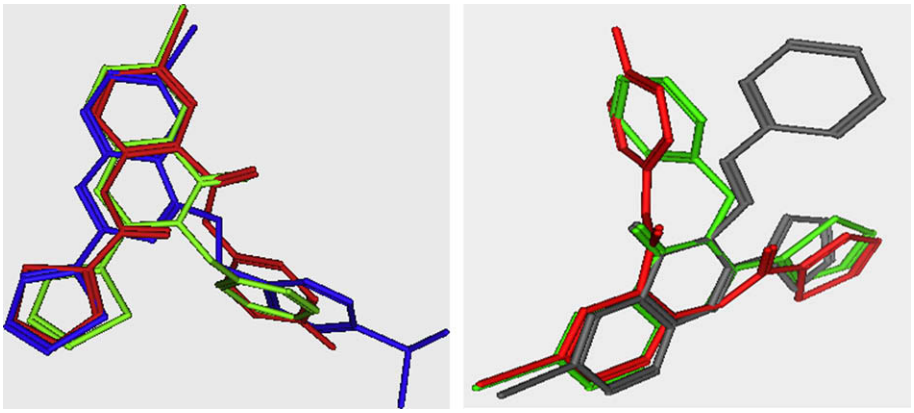

Fig. 4. Flexible alignments of the most active compounds (left panel): **16** (in red), **26** (in green) and **42** (in blue). Right panel showed the flexible alignments of the inactive compound **36** (in gray) and the active compounds **16** (in red), **26** (in green). (For interpretation of the references to color in this figure legend, the reader is referred to the web version of this article.)

4.1. Chemistry

4.1.1. 2-(2-Thienylcarbonylamino)-5-iodo-benzoic acid **8**

2-Thiophenecarbonyl chloride (7.33 g, 0.05 mol) was added dropwise to a stirred solution of 5-iodo-anthranilic acid (13.15 g, 0.05 mol) in pyridine (50 ml) and the reaction mixture was stirred at room temperature for 2 h. The reaction mixture was poured into cold 5% dilute HCl solution (100 ml). The solid obtained was filtered, washed several times with water, dried and crystallized from ethanol (Table 1). ^{1}H NMR (DMSO-d_6): δ 7.27 (t, 1H, $J = 4.0$ Hz, thiophene-H), 7.70 (d, 1H, $J = 0.5$ Hz, thiophene-H), 7.86–7.88 (dd, 1H, $J = 1.5$, $J = 8.5$ Hz, ArH), 7.91 (d, 1H, $J = 4.0$ Hz, thiophene-H),

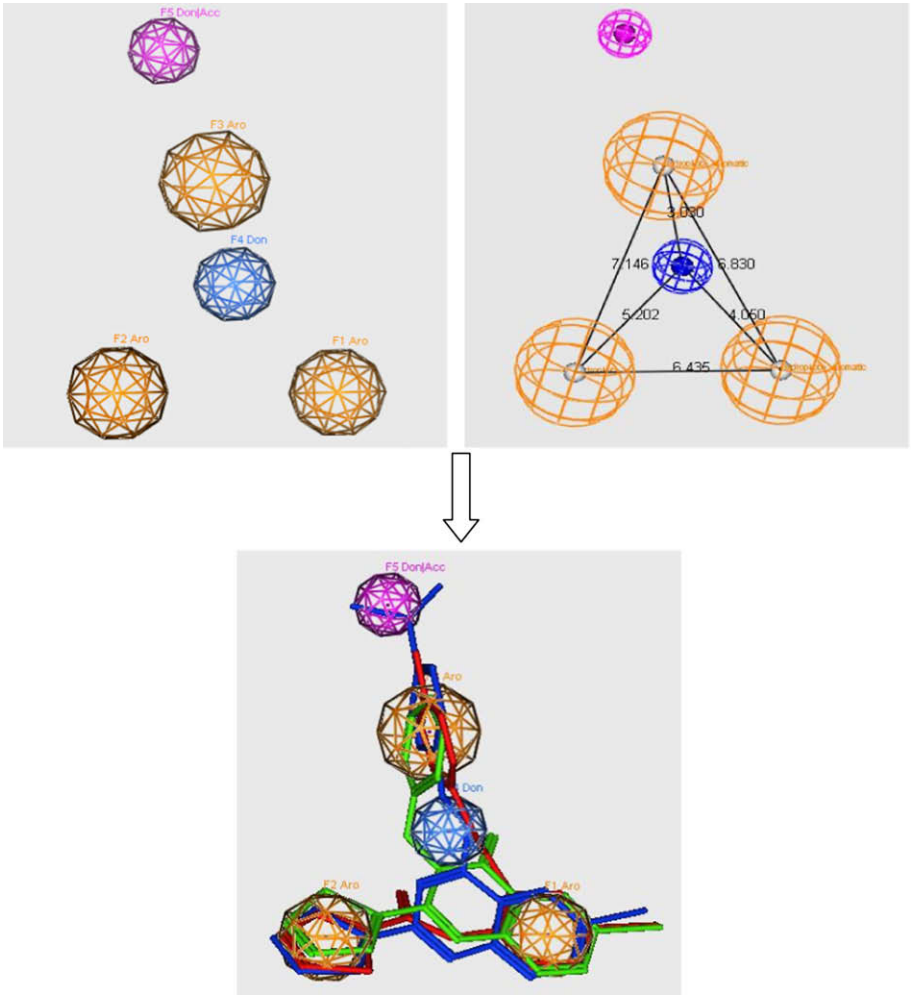

Fig. 5. The active compounds **16** (red), **26** (green) and **42** (blue), mapped to the pharmacophore model for antitumor activity. Pharmacophore features are color coded: orange for hydrophobics aromatic, blue for a hydrogen bond donor, and violet for a hydrogen bond donor/acceptor feature. The geometries of pharmacophore are shown in the upper right panel. (For interpretation of the references to color in this figure legend, the reader is referred to the web version of this article.)

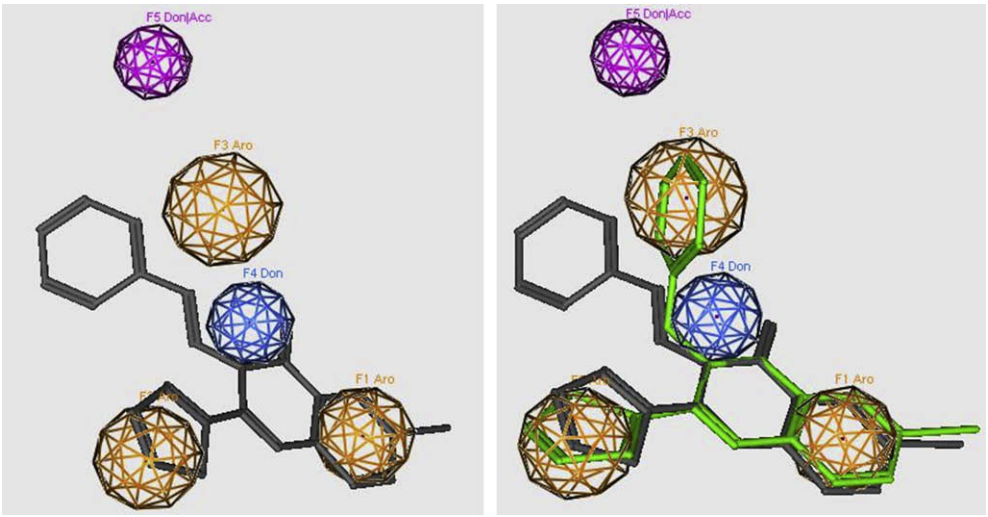

Fig. 6. The inactive compound **36**, mapped to the pharmacophore model for antitumor activity (left panel), Right panel showed that the active compound **26** (green) and in active molecule **36** (gray) are mapped together. Pharmacophore features are color coded: orange for hydrophobics aromatic, blue for a hydrogen bond donor, and violet for a hydrogen bond donor/acceptor feature. (For interpretation of the references to color in this figure legend, the reader is referred to the web version of this article.)

8.15 (d, 1H, $J = 1.5$ Hz, ArH), 8.34 (d, 1H, $J = 8.5$ Hz, ArH), 8.96 (br s, 1H, NHCO), 12.61 (s, 1H, COOH). Anal. for ($C_{12}H_8INO_3S$) C, H, N.

*4.1.2. 2-(2-Thieno)-6-iodo-4*H*-3,1-benzoxazin-4-one* ***9***

A mixture of 2-(thiophene-2-carbonylamino)-5-iodo-benzoic acid (**8**, 11.19 g, 0.03 mol) and acetic anhydride (30 g, 0.3 mol) was heated under reflux for 4 h. The solvent was removed under reduced pressure. The residue was triturated with petroleum ether 40–60. The separated solid was collected by filtration, washed with petroleum ether 40–60, dried and crystallized from toluene (Table 1). ^{1}H NMR (DMSO-d_6): δ 7.27 (t, 1H, $J = 4$ Hz, thiophene-H), 7.70 (d, 1H, $J = 0.5$ Hz, thiophene-H), 7.86–7.88 (dd, 1H, $J = 1.5$, $J = 8.5$ Hz, ArH), 7.91 (d, 1H, $J = 4.0$ Hz, thiophene-H), 8.15 (d, 1H, $J = 1.5$ Hz, ArH), 8.34 (d, 1H, $J = 8.5$ Hz, ArH). Anal. for ($C_{12}H_6INO_2S$) C, H, N.

*4.1.3. 2-(2-Thienylcarbonylamino)-5-iodo-*N*-(substituted)-benzamides* ***10–12***

A mixture of 4*H*-3,1-benzoxazin-4-one derivative (**9**, 3.55 g, 0.01 mol) and appropriate aliphatic amine (0.03 mol) in pyridine (30 ml) was heated under reflux for 3 h. The solvent was then removed under reduced pressure. The obtained solid was filtered, washed with diluted HCl and crystallized from the appropriate solvent. Yield percentage, melting points, crystallization solvent, and molecular formula are shown in Table 1. ^{1}H NMR (DMSO-d_6), **10**: δ 3.69–3.81 (q, 2H, $J = 6$ Hz, CONH–CH_2CH$_2$OH), 3.55–3.57 (q1, 2H, $J = 6$ Hz, CONH–CH$_2$$CH_2$OH), 4.80 (t, 1H, $J = 6$ Hz, OH), 7.27 (t, 1H, $J = 4$ Hz, thiophene-H), 7.70 (d, 1H, $J = 0.5$ Hz, thiophene-H), 7.86–7.88 (dd, 1H, $J = 1.5$, $J = 8.5$ Hz, ArH), 7.91 (d, 1H, $J = 4.0$ Hz, thiophene-H), 8.15 (d, 1H, $J = 1.5$ Hz, ArH), 8.34 (d, 1H, $J = 8.5$ Hz, ArH), 9.04 (s, 1H, CONH–CH$_2$), 12.57 (s, 1H, Ph–NH–CO). Anal. for ($C_{14}H_{13}IN_2O_3S$) C, H, N. **11**: δ 0.90 (5, 3H, $J = 7.5$ Hz, CH_3–CH$_2$CH$_2$NH–), 1.54–1.59 (m, 2H, $J = 7.5$, $J = 7$ Hz, CH$_3$–CH_2–CH2NH–), 3.23–3.27 (q, 2H, $J = 7$ Hz, CH$_3$–CH$_2$–CH_2–NH–), 7.27 (t, 1H, $J = 4$ Hz, thiophene-H), 7.70 (d, 1H, $J = 0.5$ Hz, thiophene-H), 7.86–7.88 (dd, 1H, $J = 1.5$, H = 8.5 Hz, ArH), 7.91 (d, 1H, $J = 4.0$ Hz, thiophene-H), 8.15 (d, 1H, $J = 1.5$ Hz, ArH), 8.34 (d, 1H, $J = 8.5$ Hz, ArH), 8.98 (s, 1H, CONH–CH$_2$), 12.59 (s, 1H, Ph–NH–CO). Anal. for ($C_{15}H_{15}IN_2O_2S$) C, H, N. **12**: δ 0.90 (t, 3H, $J = 7.5$ Hz, CH_3CH$_2$CH$_2$CH$_2$NH), 1.29–1.37 (m, 2H, $J = 7.0$, 7.5 Hz, CH$_3$–CH_2–CH$_2$–CH$_2$–NH–), 1.50–1.56 (m, 2H, $J = 7.0$, 7.5 Hz, CH$_3$CH$_2$$CH_2CH_2$NH), 3.27–3.31 (m, 2H, $J = 7.0$, $J = 7.5$ Hz, CH$_3$–CH$_2$CH$_2$$CH_2$–NH–), 7.27 (t, 1H, $J = 4$ Hz, thiophene-H), 7.70 (d, 1H, $J = 0.5$ Hz, thiophene-H), 7.86–7.88 (dd, 1H, $J = 1.5$, $J = 8.5$ Hz, ArH), 7.91 (d, 1H, $J = 4.0$ Hz, thiophene-H), 8.15 (d, 1H, $J = 1.5$ Hz, ArH), 8.34 (d, 1H, $J = 8.5$ Hz, ArH), 8.96 (s, 1H, CONH–CH$_2$–), 12.60 (s, 1H, PhNHCO–). Anal. for ($C_{16}H_{17}IN_2O_2S$) C, H, N.

*4.1.4. 2-(2-Thieno)-3-(2-chloroethyl)-4-oxo-6-iodo-*3H*-quinazoline* ***13***

A mixture of 2-(2-thienylcarbonylamino)-5-iodo-*N*-(2-hydroxyethyl)-benzamide (**10**, 4.16 g, 0.01 mol) and thionyl chloride (23.8 g, 0.2 mol) was heated under reflux for 4 h. The reaction mixture was concentrated *in vacuo* and poured into ice water. The solid obtained was crystallized from dioxane (Table 1). ^{1}H NMR; (DMSO-d_6): δ 3.87 (t, 2H, $J = 7$ Hz, N–CH_2–CH$_2$Cl), 4.5 (t, 2H, $J = 7$ Hz, NCH$_2$$CH_2$–Cl), 7.27 (t, 1H, $J = 4$ Hz, thiophene-H), 7.70 (d, 1H, $J = 0.5$ Hz, thiophene-H), 7.86–7.88 (dd, 1H, $J = 1.5$, $J = 8.5$ Hz, ArH), 7.91 (d, 1H, $J = 4.0$ Hz, thiophene-H), 8.15 (d, 1H, $J = 1.5$ Hz, ArH), 8.34 (d, 1H, $J = 8.5$ Hz, ArH). Anal. for ($C_{14}H_{10}ClIN_2OS$) C, H, N.

*4.1.5. 2-(2-Thienylcarbonylamino)-5-iodo-*N*-(4-substituted phenyl)-benzamides* ***14–18***

A mixture of compound (**9**, 3.55 g, 0.01 mol) and appropriate aromatic amines (0.20 mol) in dry pyridine (50 ml) was refluxed for 8 h. The reaction mixture was cooled and treated with acidulated ice cold water (10%). The separated product was washed several times with water and recrystallized from appropriate solvent (Table 1). ^{1}H NMR (DMSO-d_6), **14**: δ 7.16 (t, 1H, $J = 7.50$ Hz, ArH), 7.24–7.25 (m, 1H, ArH), 7.39 (t, 2H, $J = 8.0$ Hz, ArH), 7.71–7.75 (m, 3H, ArH), 7.89–7.95 (m, 2H, ArH), 8.17 (d, 1H, $J = 9.0$ Hz, ArH), 8.23 (d, 1H, $J = 1.5$ Hz, ArH), 10.62 (s, 1H, NH), 11.64 (s, 1H, NH). Anal. for ($C_{18}H_{13}IN_2O_2S$) C, H, N. **15**: δ 7.24 (t, 1H, $J = 4.50$ Hz, ArH), 7.31 (d, 2H, $J = 9.0$ Hz, ArH), 7.41–7.58 (m, 3H, ArH), 7.85–7.93 (m, 2H, ArH), 8.13 (d, 1H, $J = 9.0$ Hz, ArH), 8.2 (d, 1H, $J = 1.5$ Hz, ArH), 10.69 (s, 1H, NH), 11.52 (s, 1H, NH). Anal. for ($C_{18}H_{12}ClIN_2O_2S$) C, H, N. **16**: δ 6.77–7.75 (dd, 4H, $J = 9.0$ Hz, ArH), 7.23–7.26 (m, 1H, ArH), 7.13 (d, 1H, $J = 3.00$ Hz, ArH), 7.91–7.93 (m, 2H, ArH), 8.23–8.24 (m, 2H, ArH), 9.63 (s, 1H, OH), 10.43 (s, 1H, NH), 11.89 (s, 1H, NH). Anal. for ($C_{18}H_{13}IN_2O_3S$) C, H, N. **17**: δ 3.67 (s, 3H, OCH_3), 6.96–7.60 (dd, 4H, $J = 9.0$ Hz, ArH), 7.35 (t, 1H, $J = 4.0$ Hz, ArH), 7.7 (s, 1H, ArH), 7.90–7.92 (m, 1H, ArH), 8.19–8.23 (m, 2H, ArH), 8.37 (d, 1H, $J = 1.5$ Hz, ArH), 10.51 (br s, 1H, NH), 11.81 (br s, 1H, NH). Anal. for ($C_{19}H_{15}IN_2O_3S$) C, H, N. **18**: δ 1.32 (t, 3H, $J = 7.0$ Hz, OCH$_2$$CH_3$), 3.99–4.03 (q, 2H, $J = 7.0$, OCH$_2$$CH_3$), 6.94–7.59 (dd, 4H, $J = 9.0$ Hz, ArH), 7.24 (t, 1H, $J = 4.50$ Hz, ArH), 7.71 (d, 1H, $J = 3.50$ Hz, ArH),

7.89–7.92 (m, 3H, ArH), 8.22 (d, 1H, $J = 8$ Hz, ArH), 10.51 (s 1H, NH), 11.83 (s, 1H, NH). Anal. for ($C_{20}H_{17}IN_2O_3S$) C, H, N.

4.1.6. 2-(Thieno)-6-iodo-3-[4-(substituted sulphonamido)phenyl]-3H-quinazolin-4-one **19–22**

A mixture of compound (**9**, 3.55 g, 0.01 mol) and appropriate sulfa drug (0.01 mol) was fused at 210° in oil bath for 1 h, cooled and triturated with methanol and filtered. The resulting solid was washed several times with water, dried and recrystallized from suitable solvent to obtain compounds **19–22** (Table 1). ^{1}H NMR (DMSO-d_6), **19**: δ 7.24–7.28 (m, 2H, ArH), 7.74–7.77 (m, 2H, ArH), 7.90–7.97 (m, 3H, ArH), 8.28–8.29 (m, 2H, ArH), 8.37 (d, 1H, $J = 9.0$ Hz, ArH), 12.05 (br s, 2H, NH_2). Anal. for ($C_{18}H_{12}IN_3O_3S_2$) C, H, N. **20**: δ 6.81 (d, 1H, $J = 4.5$ Hz, thiazole-H), 7.25 (d, 1H, $J = 4.5$ Hz, thiazole-H), 7.69–7.95 (m, 10H, ArH), 10.27 (br s, 1H, NH). Anal. for ($C_{21}H_{13}IN_4O_3S_3$) C, H, N. **21**: δ 6.57 (d, 2H, $J = 8.5$ Hz, ArH), 7.01 (t, 1H, $J = 5.0$ Hz, ArH), 7.29 (t, 1H, $J = 5.0$ Hz, ArH), 7.41 (d, 1H, $J = 5.0$ Hz, ArH), 7.62 (d, 2H, $J = 8.5$ Hz, ArH), 7.86–7.88 (dd, 1H, $J = 1.5$, 8.5 Hz, ArH), 8.18–8.20 (m, 2H, ArH), 8.29 (d, 1H, $J = 8.5$ Hz, ArH), 8.35 (d, 1H, $J = 3.0$ Hz, ArH), 8.48 (d, 1H, $J = 9.0$ Hz, ArH), 11.38 (br s, 1H, NH). Anal. for ($C_{22}H_{14}IN_5O_3S_2$) C, H, N. **22**: δ 3.57 (br s, 1H, NH), 7.28 (t, 1H, $J = 5.0$ Hz, ArH), 7.39 (d, 4H, $J = 9.0$ Hz, ArH), 7.91–7.92 (m, 2H, ArH), 8.00–8.02 (m, 2H, ArH), 8.15–8.18 (m, 2H, ArH), 8.32–8.34 (m, 2H, ArH). Anal. for ($C_{19}H_{14}IN_5O_3S_2$) C, H, N.

4.1.7. 2-(2-Thieno)-6-iodo-3-(4-sulphonamido-benzyl)-3H-quinazolin-4-one **23**

Equimolar amounts of compound (**9**, 3.55, 0.01 mol) and homosulfanilamide (1.86 g, 0.01 mol) were fused together at 200° in an oil bath for 1 h. On cooling, the solid mass dissolved in hot glacial acetic acid (50 ml), and filtered. The filtrate was concentrated *in vacuo* and the resulting solid was filtered, washed with water and recrystallized to afford **23** (Table 1). ^{1}H NMR (DMSO-d_6): δ 4.50 (s, 2H, CH_2Ph), 7.25–7.27 (m, 1H, ArH), 7.34 (br s, 2H, NH_2), 7.54–7.82 (dd, 4H, $J = 8.5$ Hz, ArH), 7.68 (d, 1H, $J = 5.0$ Hz, ArH), 7.90–7.92 (m, 2H, ArH), 8.26 (d, 1H, $J = 3.0$ Hz, ArH), 8.34 (d, 1H, $J = 9.0$ Hz, ArH). Anal. for ($C_{19}H_{14}IN_3O_3S_2$) C, H, N.

4.1.8. 2-(2-Thieno)-6-iodo-3-hydroxy-3,4-dihydro-quinazolin-4-one **24**

A mixture of 2-(2-thieno)-6-iodo-4*H*-3,1-benzoxazin-4-one (**9**, 3.55, 0.01 mol) and hydroxylamine hydrochloride (0.7 g, 0.01 mol) in dry pyridine (35 ml) was heated under reflux for 8 h and the reaction mixture was then concentrated to half its volume. The separated solid was filtered, washed with water and crystallized to afford **24** (Table 1). ^{1}H NMR (DMSO-d_6): δ 5.3 (s, 1H, OH, D_2O exchanged), 7.25 (t, 1H, $J = 4$ Hz, thiophene-H), 7.70 (d, 1H, $J = 0.5$ Hz, thiophene-H), 7.86–7.88 (dd, 1H, $J = 8.5$, 1.5 Hz, ArH), 7.91 (d, 1H, $J = 4.0$ Hz, thiophene-H), 8.15 (d, 1H, $J = 1.5$ Hz ArH), 8.34 (d, 1H, $J = 8.5$ Hz, ArH). Anal. for ($C_{12}H_7IN_2O_2S$) C, H, N.

4.1.9. 2-(2-Thieno)-6-iodo-3-substitututed amino-3,4-dihydro-quinazolin-4-one **25–29**

A mixture of 2-(2-thieno)-6-iodo-4*H*-3,1-benzoxazin-4-one (**9**, 3.55 g, 0.01 mol) and the required hydrazine derivative or benzoic acid hydrazide (0.012 mol) in *n*-butanol (20 ml) was heated under reflux for 6 h. The reaction mixture was concentrated, cooled and the separated solid was crystallized out from the proper solvent to afford compounds **25–29** (Table 1). ^{1}H NMR (DMSO-d_6), **25**: δ 5.7–5.8 (br s, 2H, NH_2, D_2O exchanged), 7.27 (t, 1H, $J = 4$ Hz, thiophene-H), 7.73 (d, 1H, $J = 0.5$ Hz, thiophene-H), 7.85–7.87 (dd, 1H, $J = 8.5$, 1.5 Hz, ArH), 7.92 (d, 1H, $J = 4.0$ Hz, thiophene-H), 8.1 (d, 1H, $J = 1.5$ Hz, ArH), 8.33 (d, 1H, $J = 8.5$ Hz, ArH). Anal. for ($C_{12}H_8IN_3OS$) C, H, N. **26**: 6.75 (t, 1H, $J = 7.5$ Hz, ArH), 6.84 (d, 2H, $J = 8$ Hz, ArH), 7.17 (t, 1H, $J = 8$ Hz, ArH), 7.22 (t, 1H, $J = 4$ Hz, thiophene-H), 7.66 (d, 1H, $J = 3$ Hz, thiophene-H), 7.91 (d, 1H, $J = 5$ Hz, thiophene-H), 7.94–7.96 (dd, 1H, $J = 8.5$, 1.5 Hz, quinazoline-H), 8.02 (s, 1H, quinazoline-H), 8.28 (d, 1H, $J = 8.5$ Hz, quinazoline-H), 8.31 (d, 1H, $J = 2$H, ArH), 10.7 (s, 1H, NH). Anal. for ($C_{18}H_{12}IN_3OS$) C, H, N. **27**: δ 6.78 (d, 2H, $J = 9$ Hz, ArH), 7.17–7.19 (m, 1H, $J = 4.1$ Hz, thiophene-H), 7.23 (d, 2H, $J = 9$ Hz, ArH), 7.55 (d, 1H, $J = 9$ Hz, thiophene-H), 7.83–7.84 (dd, 1H, $J = 3.5$, 1.5 Hz, thiophene-H), 8.14–8.17 (dd, 1H, $J = 6.5$, 2 Hz, quinazoline-H), 8.24–8.25 (dd, 1H, $J = 2.5$, 1.5 Hz, quinazoline-H), 8.35 (d, 1H, $J = 2$ Hz, quinazoline-H), 9.6 (s, 1H, NH). Anal. for ($C_{18}H_{11}ClIN_3OS$) C, H, N. **28**: δ 7.27 (t, 1H, $J = 4$ Hz, thiophene-H), 7.34–8.34 (m, 8H, ArH), 9.5 (s, 1H, NH). Anal. for ($C_{18}H_{10}IN_5O_5S$) C, H, N. **29**: δ 7.24 (t, 1H, $J = 4$ Hz, thiophene-H), 7.41–8.35 (m, 10 H, ArH), 12.31 (br s, 1H, NHC=O, D_2O exchanged). Anal. for ($C_{19}H_{12}IN_3O_2S$) C, H, N.

4.1.10. 2-(2-Thieno)-6-iodo-3,4-dihydro-quinazolin-4-one **30**

A mixture of 2-(thieno)-6-iodo-4*H*-3,1-benzoxazin-4-one (**9**, 3.55 g, 0.01 mol) and formamide (30 ml) was heated under reflux for 3 h. On cooling, the separated solid was filtered, washed with water and crystallized from acetic acid to yield **30** (Table 1). ^{1}H NMR (DMSO-d_6): δ 7.25 (t, 1H, $J = 4$ Hz, thiophene-H), 7.70 (d, 1H, $J = 0.5$ Hz, thiophene-H), 7.86–7.88 (dd, 1H, $J = 8.5$, 1.5 Hz, quinazoline-H), 7.91 (d, 1H, $J = 4.0$ Hz, thiophene-H), 8.15 (d, 1H, $J = 1.5$ Hz, quinazoline-H), 8.34 (d, 1H, $J = 8.5$ Hz, quinazoline-H), 12.7 (br s, 1H, NH). Anal. for ($C_{12}H_7IN_2OS$) C, H, N.

4.1.11. 2-(2-Thieno)-6-iodo-3,4-dihydro-quinazolin-4-thione **31**

Phosphorous pentasulfide (2.31 g, 0.011 mol) was added to a solution of 2-(2-thieno)-6-iodo-3,4-dihydro-quinazolin-4-one (**30**, 3.54 g, 0.01 mol) in xylene (30 ml), and the mixture was heated under reflux for 3 h, then filtered while hot. On cooling, the obtained solid was filtered, and washed with water, dried and crystallized from acetic acid to give **31** (Table 1). ^{1}H NMR (DMSO-d_6): δ 7.24 (t, 1H, $J = 4$ Hz, thiophene-H), 7.70 (d, 1H, $J = 0.5$ Hz, thiophene-H), 7.86–7.88 (dd, 1H, $J = 8.5$, 1.5 Hz, quinazoline-H), 7.91 (d, 1H, $J = 4.0$ Hz, thiophene-H), 8.15 (d, 1H, $J = 1.5$ Hz, quinazoline-H), 8.34 (d, 1H, $J = 8.5$ Hz, quinazoline-H), 12.5 (br s, NH, exchanged). Anal. for ($C_{12}H_7IN_2S_2$) C, H, N.

4.1.12. 2-(2-Thieno)-4-alkylthio-6-iodo-quinazolines **32**, **33**

A mixture of 2-(2-thieno)-6-iodo-3,4-dihydro-quinazoline-4-thione (**31**, 3.7 g, 0.01 mol), the appropriate alkyl halide (0.015 mol) and anhydrous potassium carbonate (2 g) in dry acetone (50 ml) was heated under reflux for 3 h and the reaction mixture was filtered while hot. The filtrate was evaporated under vacuum and the separated solid was washed with water and crystallized from ethanol to give **32**, **33** (Table 1). ^{1}H NMR (DMSO-d_6), **32**: δ 2.64 (s, 3H, SCH_3), 7.27 (t, 1H, $J = 4$ Hz, thiophene-H), 7.70 (d, 1H, $J = 0.5$ Hz, thiophene-H), 7.86–7.88 (dd, 1H, $J = 8.5$, 1.5 Hz, quinazoline-H), 7.91 (d, 1H, $J = 4.0$ Hz, thiophene-H), 8.15 (d, 1H, $J = 1.5$ Hz, quinazoline-H), 8.34 (d, 1H, $J = 8.5$ Hz, quinazoline-H). Anal. for ($C_{13}H_9IN_2S_2$) C, H, N. **33**: δ 1.2–1.3 (t, 3H, $J = 10$ Hz, CH_3–CH_2–) 3.01–3.02 (q, 2H, $J = 10$ Hz, CH_3–CH–), 7.27 (t, 1H, $J = 4$ Hz, thiophene-H), 7.70 (d, 1H, $J = 0.5$ Hz, thiophene-H), 7.86–7.88 (dd, 1H, $J = 1.5$ Hz, quinazoline-H), 7.91 (d, 1H, $J = 4.0$ Hz, thiophene-H), 8.15 (d, 1H, $J = 1.5$ Hz, quinazoline-H), 8.34 (d, 1H, $J = 8.5$ Hz, quinazoline-H). Anal. for ($C_{14}H_{11}IN_2S_2$) C, H, N.

4.1.13. N-(Phenyl)-N′-[2-(2-thieno)-4-oxo-6-iodo-3H-quinazolin-3-yl]-urea (**34**) and thiourea **35**

A mixture of 2-(2-thieno)-6-iodo-3-amino-quinazolin-4-one (**25**, 3.69 g, 0.01 mol), phenylisocyanate or phenylisothiocyanate (0.015 mol) in dry dioxane (30 ml) was refluxed for 8 h. The excess solvent was removed and the solid was crystallized from the proper solvent to give compounds **34**, **35,** respectively (Table 1). ^{1}H NMR (DMSO-d_6), **34**: δ 6.75 (t, 1H, $J = 7.5$ Hz ArH), 6.84 (d, 2H, $J =$ Hz, ArH), 7.17 (t, 2H, $J = 7.5$ Hz, ArH), 7.22 (t, 1H, $J = 4$ Hz, thiophene-H), 7.7 (d, 1H, $J = 2$ Hz, thiophene-H), 7.85 (d, 1H, $J = 5$ Hz, thiophene-H), 7.94–7.96 (dd, 1H, $J = 7$, 2 Hz, quinazoline-H), 8.15 (d, 1H, 1.5 Hz,

quinazoline-H), 8.34 (d, 1H, 7.5 Hz, quinazoline-H), 10.7 (s, 1H, =N–*NH*–CO), 12.05 (s, H, CO*NH*Ph). Anal. for ($C_{19}H_{13}IN_4O_2S$) C, H, N. **35**: δ 6.76 (t, 1H, $J = 7.5$ Hz, ArH), 6.84 (d, 2H, $J = 8$ Hz, ArH), 7.17 (t, 2H, $J = 7.5$, ArH), 7.22 (t, 1H, $J = 4$ Hz, thiophene-H), 7.7 (d, 1H, $J = 2$ Hz, thiophene-H), 7.85 (d, 1H, $J = 5$ Hz, thiophene-H), 7.93–7.95 (dd, $J = 7$, 2 Hz, quinazoline-H), 8.09 (d, 1H, 1.5 Hz, quinazoline-H), 8.33 (d, 1H, 7.5 Hz, quinazoline-H), 11.7 (s, 1H, =N–*NH*–CS–), 12.7 (s, H, CS*NH*Ph). Anal. for ($C_{19}H_{13}IN_4OS_2$) C, H, N.

4.1.14. 2-(2-Thieno)-3-arylideneamino-6-iodo-3,4-dihydro-quinazolin-4-ones **36**, **37**

A mixture of 2-(2-thieno)-3-amino-3,4-dihydro-quinazolin-6-one (**25**, 3.69 g, 0.01 mol) and the appropriate aldehyde (0.015 mol) in glacial acetic acid (130 ml) was heated under reflux for 8 h. On cooling, the separated solid was filtered, washed with water and crystallized from acetic acid to give **36**, **37** (Table 1). ^{1}H NMR (DMSO-d_6), **36**: δ 7.23 (t, 1H, $J = 4$ Hz, thiophene-H), 7.3 (m, 3H, ArH), 7.6 (d, 2H, $J = 7$ Hz, ArH), 7.70 (d, 1H, $J = 0.5$ Hz, thiophene-H), 7.86–7.88 (dd, 1H, $J = 8.5$, 1.5 Hz, quinazoline-H), 7.91 (d, 1H, $J = 4.0$ Hz, thiophene-H), 8.15 (d, 1H, $J = 1.5$ Hz, quinazoline-H), 8.34 (d, 1H, $J = 8.5$ Hz, quinazoline-H), 9.25 (s, 1H, CH=N). Anal. for ($C_{19}H_{12}IN_3OS$) C, H, N. **37**: δ 3.73 (s, 3H, O*CH*$_3$), 6.8 (d, 2H, $J = 8$ Hz, ArH), 7.23 (t, 1H, $J = 4.0$ Hz, thiophene-H), 7.5 (d, 2H, $J = 8$ Hz, ArH), 7.70 (d, 1H, $J = 0.5$ Hz, thiophene-H), 7.86–7.88 (dd, 1H, $J = 8.5$, 1.5 Hz, quinazoline-H), 7.91 (d, 1H, $J = 4.0$ Hz, thiophene-H), 8.15 (d, 1H, $J = 1.5$ Hz, quinazoline-H), 8.34 (d, 1H, $J = 8.5$ Hz, quinazoline-H), 9.22 (s, 1H, CH=N). Anal. for ($C_{20}H_{14}IN_3O_2S$) C, H, N.

4.1.15. 2-(2-Thieno)-3-(3-oxobutyryl)amino-6-iodo-3,4-dihydro-quinazolin-3-one **38**

A mixture of 2-(2-thieno)-6-iodo-3-amino-quinazolin-4-one (**25**, 3.69 g, 0.01 mol) and ethyl acetoacetate (0.03 mol) in isopropanol (30 ml), was heated under reflux for 18 h. The reaction mixture was concentrated to third its volume. The separated solid was filtered, washed with water and crystallized from ethanol to give **38** (Table 1). ^{1}H NMR ($CDCl_3$), δ 2.2 (s, 3H, CO*CH*$_3$), 3.6 (s, 2H, CO*CH*$_2$CO–), 7.25 (t, 1H, $J = 4.0$ Hz, thiophene-H), 7.70 (d, 1H, $J = 0.5$ Hz, thiophene-H), 7.86–7.88 (dd, 1H, $J = 8.5$, 1.5 Hz, quinazoline-H), 7.91 (d, 1H, $J = 4.0$ Hz, thiophene-H), 8.15 (d, 1H, $J = 1.5$ Hz, quinazoline-H), 8.34 (d, 1H, $J = 8.5$ Hz, quinazoline-H), 10.7 (s, 1H, =N–*NH*CO–). Anal. for ($C_{16}H_{12}IN_3O_3S$) C, H, N.

4.1.16. 2-(2-Thieno)-4-(ethoxycarbonylmethyloxy)-6-iodo-3,4-dihydro-quinazoline **39**

A mixture of 2-(2-thieno)-6-iodo-3,4-dihydro-quinazolin-3-one (**30**, 3.54 g, 0.01 mol), ethylbromoacetate (0.015 mol) and anhydrous potassium carbonate (2.0 g) in dry acetone (50 ml) was heated under reflux for 12 h. The reaction mixture was filtered while hot and the filtrate was concentrated *in vacuo* to give the crude product which was crystallized from ethanol to give **39** (Table 1). ^{1}H NMR ($CDCl_3$), δ 1.2 (t, 3H, $J = 7$ Hz, *CH*$_3$CH$_2$–), 4.17–4.21 (q, 2H, $J = 7$ Hz, CH$_3$*CH*$_2$–), 5.22 (s, 2H, O*CH*$_2$CO–), 7.23 (t, 1H, $J = 5.0$ Hz, thiophene-H), 7.70 (d, 1H, $J = 1.5$ Hz, thiophene-H), 7.81–7.83 (dd, 1H, $J = 8.5$, 1.5 Hz, quinazoline-H), 7.94–7.95 (d, 1H, $J = 5$ Hz, thiophene-H), 8.18–8.20 (d, 1H, $J = 1.5$ Hz, quinazoline-H), 8.44 (d, 1H, $J = 8.5$ Hz, quinazoline-H). Anal. for ($C_{16}H_{13}IN_2O_3S$) C, H, N.

4.1.17. 4-[2-(2-Thieno)-6-iodo-3H-quinazolin-4-yl-oxy]-acetyl hydrazine **40**

A solution of the synthesized ester **39** (0.01 mol) and hydrazine hydrate (85%, 5 ml) in ethanol (50 ml) was heated under reflux for 3 h. The solvent was evaporated and the obtained residue was recrystallized from dioxane to give **40** (Table 1). ^{1}H NMR (DMSO-d_6): δ 5.1 (s, 2H, *CH*$_2$CO–), 4.29 (br s, 2H, NH$_2$), 7.17–7.19 (t, 1H, $J = 4.0$ Hz, thiophene-H), 7.43–7.45 (d, 1H, $J = 0.5$ Hz, thiophene-H), 7.7–7.71 (dd, 1H, $J = 8.5$, 1.5 Hz, quinazoline-H), 7.95–7.97 (d, 1H, $J = 4.0$ Hz, thiophene-H), 8.04–8.05 (d, 1H, $J = 8$, 1.5 Hz, quinazoline-H), 8.5 (d, 1H, $J = 8.5$ Hz, quinazoline-H), 9.42 (br s, 1H, NH). Anal. for ($C_{14}H_{11}IN_4O_2S$) C, H, N.

4.1.18. 2-(2-Thieno)-4-chloro-6-iodo-quinazoline **41**

A mixture of 2-(2-thieno)-6-iodo-3,4-dihydro-quinazoline (**30**, 1.18 g, 0.03 mol), phosphorous oxychloride (5 g, 0.033 mol) and phosphorous pentachloride (1.01 g, 0.05 mol) was heated under reflux in an oil bath for 3 h. The excess phosphorous oxychloride was removed under reduced pressure and crushed ice (30 g) was added to the residue. The separated solid was filtered, washed with water, dried and crystallized from toluene to give **41** (Table 1). ^{1}H NMR ($CDCl_3$): δ 7.25 (t, 1H, $J = 4$ Hz, thiophene-H), 7.8 (d, 1H, $J = 1.0$ Hz, thiophene-H), 7.89–7.91 (dd, 1H, $J = 8$, 1.5 Hz, quinazoline-H), 8.06 (d, 1H, $J = 4$ Hz, thiophene-H), 8.35 (d, 1H, $J = 1.5$ Hz, quinazoline-H), 8.55 (d, 1H, $J = 8$ Hz, quinazoline-H). Anal. for ($C_{12}H_6ClIN_2S$) C, H, N.

4.1.19. 2-(2-Thieno)-4-[4-sulfonamidobenzylamino]-6-iodo-quinazoline **42**

A mixture of 2-(2-thieno)-4-chloro-6-iodo-quinazoline **41** (1.116 g, 0.003 mol) and homosulfanilamide (0.6 g, 0.003 mol) in pyridine (20 ml) was refluxed for 6 h. The solvent was then evaporated under vacuum. The residue was triturated with dilute hydrochloric acid. The obtained solid was filtered, washed with water and crystallized from dioxane to afford **42** (Table 1). ^{1}H NMR (DMSO-d_6): δ 4.6 (s, 2H, CH$_2$Ph), 7.26–7.28 (m, 1H, ArH), 7.36 (br s, 2H, NH$_2$), 7.56–7.84 (dd, 4H, $J = 8.5$ Hz, ArH), 7.68 (d, 1H, $J = 5.9$ Hz, ArH), 7.90–7.92 (m, 2H, ArH), 8.26 (d, 1H, $J = 4.5$ Hz, ArH), 8.34 (d, 1H, $J = 9.0$ Hz, ArH), 9.52 (br s, 1H, NH). Anal. for ($C_{19}H_{15}IN_4O_2S_2$) C, H, N.

4.1.20. 2-(2-Thieno)-4[4-substituted sulfonamido-phenylamino]-6-iodo-quinazoline **43**–**45**

A mixture of 2-(2-thieno)-4-chloro-6-iodo-quinazolin **41** (1.12 g, 0.003 mol) and appropriate sulfa drug (0.003 mol) in dry pyridine (20 ml) was heated under reflux for 18 h. The solvent was removed under vacuum and the separate solid was filtered, washed with water, dried and recrystallized from suitable solvent to obtain compounds **43**–**45** (Table 1). ^{1}H NMR (DMSO-d_6), **43**: δ 7.25–7.29 (m, 2H, ArH), 7.75–7.77 (m, 2H, ArH), 7.90–7.97 (m, 3H, ArH), 8.28–8.29 (m, 2H, ArH), 8.37 (d, 1H, $J = 9.0$ Hz, ArH), 9.61 (br s, 1H, NH), 12.12 (br s, 2H, NH$_2$). Anal. for ($C_{18}H_{13}IN_4O_2S_2$) C, H, N. **44**: δ 6.82 (d, 1H, $J = 4.5$ Hz, thiazole-H), 7.25 (d, 1H, $J = 4.5$, thiazole-H), 7.69–7.95 (m, 10H, ArH), 9.52 (br s, 1H, NH), 10.37 (br s, 1H, NH). Anal. for ($C_{21}H_{14}IN_5O_2S_3$) C, H, N. **45**: δ 6.6 (d, 2H, $J = 8.0$ Hz, ArH), 7.06 (t, 1H, $J = 5.0$ Hz, ArH), 7.29 (t, 1H, $J = 5.0$ Hz, ArH), 7.41 (d, 1H, $J = 5.0$ Hz, ArH), 7.62 (d, 2H, $J = 8.0$ Hz, ArH), 7.85–7.87 (dd, 1H, $J = 1.5$, 8 Hz, ArH), 8.16–8.18 (m, 2H, ArH), 8.29 (d, 1H, $J = 8$ Hz, ArH), 8.36 (d, 1H, $J = 3.0$ Hz, ArH), 8.49 (d, 1H, $J = 8.0$ Hz, ArH), 9.57 (br s, 1H, NH), 10.61 (br s, 1H, NH). Anal. for ($C_{22}H_{15}IN_6O_2S_2$) C, H, N.

4.2. Antitumor screening

Under a sterile condition, cell lines were grown in RPMI 1640 media (Gibco, NY, USA) supplemented with 10% fetal bovine serum (Biocell, CA, USA); 5×10^5 cell/ml was used to test the growth inhibition activity of the synthesized compounds. The concentrations of the compounds ranging from 0.01 to 100 μM were prepared in phosphate buffer saline. Each compound was initially solubilized in dimethyl sulfoxide (DMSO), however, each final dilution contained less than 1% DMSO. Solutions of different concentrations (0.2 ml) were pipetted into separate well of a microtiter tray in duplicate. Cell culture (1.8 ml) containing a cell population of 6×10^4 cells/ml was pipetted into each well. Controls, containing only phosphate buffer saline and DMSO at identical dilutions, were also prepared in the same manner. These cultures were incubated in a humidified incubator at 37 °C. The incubator was supplied with 5% CO_2 atmosphere.

After 48 h, cells in each well were diluted 10 times with saline and counted by using a coulter counter. The counts were corrected for the dilution.

4.3. Molecular modeling methods

4.3.1. Conformational search

Initial structures for the active molecules **16**, **19**, **20**, **24**, **26**, **29**, **35**, **38**, **40**, **42** and **44**, and the inactive molecules **12**, **23**, **25**, **33** and **36** were constructed using the HyperChem program version 5.1. The MM^{+} (calculations *in vacuo*, bond dipole option for electrostatics, Polake–Ribiere algorithm, and RMS gradient of 0.01 kcal/Å mol) conformational searching in torsional space was performed using the multiconformer method [36]. Energy minima for the above compounds were determined by a semi-empirical method AM1 (as implemented in HyperChem 5.1). The conformations thus obtained were confirmed as minima by vibrational analysis. Atom-centred charges for each molecule were computed from the AM1 wave functions (HyperChem 5.1) by the procedure of Orozco and Luque [37], which provides derived charges that resemble those obtainable from ab initio 6-31G* calculations. 3D-Pharmacophore calculation was performed by MOE 2007.09 molecular modeling software [34].

4.3.2. Flexible alignment and pharmacophore prediction

Flexible alignment and pharmacophore prediction of compounds **16**, **26**, **42** and **36** were carried out with the software 'Molecular Operating Environment' (MOE of Chemical Computing Group Inc., on a Core 2 duo 1.83 GHz workstation). The molecules were built using the Builder module of MOE. Their geometry was optimized by using the MMFF94 force-field followed by a flexible alignment using systematic conformational search. Lowest energy aligned conformation(s) were identified through the analysis module of DSV by Accelrys Inc., [38] and the distances and angles between the pharmacophoric elements were measured.

Acknowledgments

The financial support of King Abdulaziz City for Science and Technology, Grant APR-23-39, is acknowledged. Thanks are due to the NCI, Bethesda, MD, for performing the antitumor testing of the synthesized compounds. Our sincere acknowledgments to Chemical Computing Group Inc, 1010 Sherbrooke Street West, Suite 910, Montreal, H3A 2R7, Canada., for their valuable agreement to evaluate the package of MOE 2007.09 software. The technical assistance of Mr. Tanvir A. Butt is greatly appreciated.

References

[1] V. Bavetsias, J.H. Marriott, C. Melin, R. Kimbell, Z.S. Matusia, F.T. Boyle, A.L. Jackman, J. Med. Chem. 43 (2000) 1910–1926.
[2] J.B. Smaill, G.W. Rewcastle, J.A. Loo, K.D. Gries, O.H. Chan, E.L. Reyner, E. Lipka, H.D. Showalter, P.W. Vincent, W.L. Elliot, W.A. Denny, J. Med. Chem. 43 (2000) 1380–1397.
[3] A. Wissner, D.M. Berger, D.H. Boschelli, M.B. Floyd, L.M. Greenbertger, H. Tsou, E. Upeslacis, Y.F. Wang, N. Zhang, J. Med. Chem. 43 (2000) 3244–3256.
[4] H.J. Park, Y.S. Kim, J.S. Kim, E.J. Lee, Y.J. Yi, H.J. Hwang, M.E. Suh, C.K. Ryu, S.K. Lee, Bioorg. Med. Chem. Lett. 14 (2004) 3385–3388.
[5] Z. Ma, Y. Hano, T. Nomura, Y. Chen, Bioorg. Med. Chem. Lett. 14 (2004) 1193–1196.
[6] N. Malecki, P. Carato, B. Riao, J.F. Goosens, R. Houssin, C. Bailly, J.P. Henichart, Bioorg. Med. Chem. 12 (2004) 641–647.
[7] V.M. Sharma, P. Prasana, K.V. Adi Seshu, C.L.L. Rao, G.S. Kumar, C.P. Narasimhulu, P.A. Babu, R.C. Puranik, D. Subramanyam, A.V. Warlu, S. Rajagopal, K.B.S. Kumar, R. Ajaykumar, R. Rajagopalan, Bioorg. Med. Chem. Lett. 12 (2002) 2303–2307.
[8] A.M.F. Kersemaekers, G.J. Fleuren, E.G. Kenter, L.J. Van den Broek, S.M. Uljee, J. Hermans, M.J. Van de Vijver, Clin. Cancer Res. 5 (1999) 577–586.
[9] M. Maurizi, G. Almadori, G. Ferrandina, M. Distefano, M.E. Romanni, G. Cadoni, P. Benedetti-Panici, G. Paludetti, G. Scambia, S. Mancuso, Br. J. Cancer 74 (1996) 1253–1257.
[10] A.L. Harries, Int. J. Radiat. Biol. 48 (1985) 675–690.
[11] A.M. Thompson, A.J. Bridges, D.W. Fry, A.J. Kraker, W.A. Denny, J. Med. Chem. 38 (1995) 3780–3788.
[12] A.J. Bridges, H. Zhou, D.R. Cody, G.W. Rewcastle, A. McMichael, H.D. Showalter, D.W. Fry, A.J. Kraker, W.A. Denny, J. Med. Chem. 39 (1996) 267–276.
[13] A.E. Wakeling, A.J. Barker, D.H. Davies, D.S. Brown, L.R. Green, S.A. Cartlidge, J.R. Woodburn, Breast Cancer Res. Treat. 38 (1996) 67–73.
[14] R.J. Griffin, S. Srinivasan, K. Bowman, A.H. Calvert, N.J. Curtin, D.R. Newell, L.C. Pemberton, B.T. Golding, J. Med. Chem. 41 (1998) 5247–5256.
[15] S.G. Abdel Hamide, H.A. El-Obeid, K.A. Al-Rashood, A.A. Khalil, H.I. El-Subbagh, Sci. Pharm. 69 (2001) 351–366.
[16] A.A. Khalil, S.G. Abdel Hamide, A.M. Al-Obaid, H.I. El-Subbagh, Arch. Pharm. Pharm. Med. Chem. 336 (2003) 95–103.
[17] H.I. El-Subbagh, S.M. Abu-Zaid, M.A. Mahran, F.A. Badria, A.M. Al-Obaid, J. Med. Chem. 43 (2000) 2915–2921.
[18] H.I. El-Subbagh, A.M. Al-Obaid, Eur. J. Med. Chem. 31 (1996) 1017–1021.
[19] H.I. El-Subbagh, M.A. El-Sherbeny, M.N. Nasr, F.E. Goda, F.A. Badria, Boll. Chim. Farm. 134 (1995) 80–84.
[20] H.I. El-Subbagh, W.A. El-Naggar, F.A. Badria, Med. Chem. Res. 3 (1994) 503–516.
[21] M.R. Grever, S.A. Schepartz, B.A. Chabner, Semin. Oncol. 19 (1992) 622–638.
[22] A. Monks, D. Scudiero, P.J. Skehan, J. Natl. Cancer Inst. 83 (1991) 757–766.
[23] M.R. Boyd, K.D. Paull, Drug Rev. Res. 34 (1995) 91–109.
[24] P. Skehan, R. Storeng, D. Scudiero, A. Monks, J. McMahon, D. Vistica, J.R. Warren, H. Bokesch, S. Kenney, M.R. Boyd, J. Natl. Cancer Inst. 82 (1990) 1107–1112.
[25] S. Profeta, N.L. Allinger, J. Am. Chem. Soc. 107 (1985) 1907–1918.
[26] HyperChem: Molecular Modeling System, Hypercube, Inc., Release 5.1, Florida, USA, 1997.
[27] M.J.S. Dewar, E.G. Zoebisch, E.F. Healy, J.J.P. Stewart, J. Am. Chem. Soc. 107 (1985) 3902–3909.
[28] U. El-Ayaan, A.A.-M. Abdel-Aziz, S. Al-Shihry, Eur. J. Med. Chem. 42 (2007) 1325–1333.
[29] A.A.-M. Abdel-Aziz, Eur. J. Med. Chem. 42 (2007) 614–626.
[30] S.T. Al-Rashood, I.A. Aboldahab, M.N. Nagi, L.A. Abouzeid, A.A.M. Abdel-Aziz, S.G. Abdel-Hamide, K.M. Youssef, A.M. Al-Obaid, H.I. El-Subbagh, Bioorg. Med. Chem. 14 (2006) 8608–8621.
[31] P. Labute, C. Williams, M. Feher, E. Sourial, J.M. Schmidt, J. Med. Chem. 44 (2001) 1483–1490.
[32] S. Kearsley, Tetrahedron Comput. Methodol. 3 (1990) 615–633.
[33] W. Gerhard, S. Thomas, B. Fabian, L. Thierry, Drug Discovery Today 13 (2008) 23–29.
[34] MOE 2007.9 of Chemical Computing Group. Inc.
[35] T.A.J. Halgren, J. Comput. Chem. 17 (1996) 490–519.
[36] M. Lipton, W.C.J. Still, J. Comput. Chem. 9 (1988) 343–355.
[37] M. Orozco, F.J.J. Luque, J. Comput. Chem. 11 (1990) 909–923.
[38] DSV 2008 by Accelrys Software Inc.